

1. BIOMASS BURNINGS AND REMOTE SENSING

1.1. Role of satellite observations in describing fires

Fire is the main cause of forest destruction in countries of the Mediterranean Basin. About 50,000 fires sweep through 7,000 to 10,000 km² of Mediterranean forests, wooded lands, and other lands each year, causing enormous economic and ecological damage as well as loss of human life (FAO, 2008). Forest fire is one of the most important factors that threaten forests in Turkey, a country situated in the Mediterranean Climatic Zone. In Turkey, the coast line, which starts from Hatay and extends over the Mediterranean and Aegean up to İstanbul, has the highest fire risk. In other words, approximately 60% (12 million ha) of Turkey's forest area is located in fire sensitive areas (JRC, 2008).

Nowadays, fires are mostly ignited by humans, either on purpose in some agricultural practices or inadvertently. The fire size depend on the amount of organic material available but also by natural climatic and orographic factors. For these reasons the fire regimes are extremely variable from region to region and with large seasonal and inter-annual variability.

For the majority of the countries, very few informations are available on fire frequencies, location and extension, for few of them the only available information about fire frequencies it has been primarily related to wild fires, which are those reported by forest agencies on the provincial and regional level (most of the time difficult to obtain and often not digitized). But biomass burning is a broader phenomenon. For example, at the end of the summer, it is common practice in agricultural regions in the mid-latitudes, to burn croplands after the harvest.

Satellite remote sensing provides automated powerful means of locating and characterizing open vegetation burnings. Remote sensing observations, in contrast to forest agency reports, are not selective in the type of fire observed and recorded. If the signal is strong enough to make it observable by a satellite platform, an agricultural fire will be recorded as well as a forest fire.

It is important for decision makers to be aware that satellites can be used to continuously monitor biomass burning. To achieve even a fraction of the satellite fire product coverage in remote areas with continual monitoring by ground and aircraft observations quickly becomes more expensive than satellite monitoring. For all these reasons, in the end, satellite observations can provide a better understanding of fire issues.

The role of satellite observations for the management of forest fires has considerably increased during the last twenty years as the spatial, spectral and temporal characteristics of the sensors have been constantly improving, and new methods for the exploitation of satellite data have been developed.

Three main topics can be distinguished, in which remote sensing provides results that can be applied directly to the subject of forest fires:

- Risk of fire spreading;
- Fire detection and monitoring;
- Cartography of affected areas.

1.2. Risk of Fire Spreading

Fire Danger is a relative index of how easy it is to ignite vegetation, how difficult a fire may be to control, and how much damage a fire may do. Early warning of these conditions allows fire managers to implement fire prevention, detection, and pre-suppression action plans before fire problems begin. Fire danger information is often enhanced with satellite data, such as hot spots for early fire detection.

Normally, fire danger rating systems provide a 4- to 6-hour early warning of the highest fire danger for any particular day that the weather data is supplied. However, by using forecasted conditions from advanced numerical weather models, extended early warning (i.e., 1-2 weeks) can be provided. This extra time allows for greater coordination of resource-sharing and mobilization within and between countries.

Fire danger rating research has been ongoing since the 1920's, resulting in operational fire danger rating systems being available for about 4 decades in Canada (Stocks et al., 1989), the United States (Deeming et al., 1977), and Australia (Luke and

McArthur, 1978). Numerous other weather-based systems and indices have been developed worldwide, although the Canadian Forest Fire Weather Index (FWI) System remains the most widely used fire danger rating system internationally.

The fire danger indicators currently presented on the Global Early Warning System for Wildland Fire (Global EWS, <http://www.fire.uni-freiburg.de/gwfews/index.html>) are components of the Canadian Forest Fire Weather Index System (figure 1). The Global EWS provides 1-7 day forecasted FWI System data based on the U.S. National Centers for Environmental Prediction (NCEP) Global Forecast System. The FWI System components are currently calibrated to commonly used threshold values that identify low to extreme conditions.

However, a single fire danger value has different meaning (in a fire management context) in different parts of the world because of differences in the local fire regime. For that reason, there is additional value in understanding fire danger in relation to the ‘local’ fire regime, which includes the influences of fuel, ignition sources, climate, fire management/suppression policy, etc.

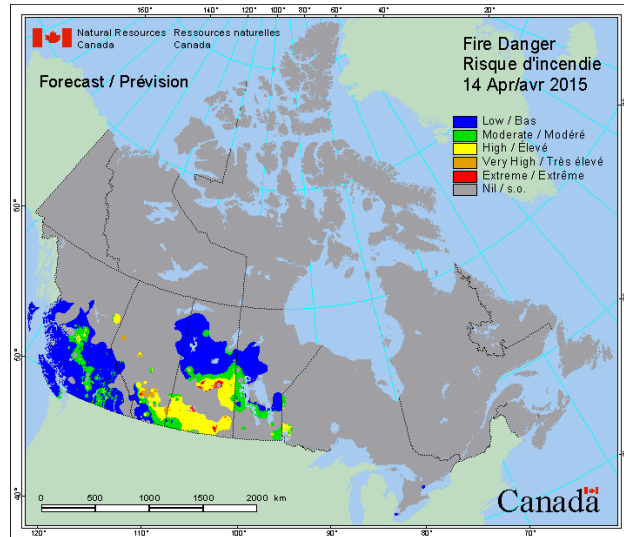


Figure 1: Fire danger level in Canada, 14 April 2015.

1.3. Fire Detection and Monitoring

By fire detection, it is understood the task of determining the location of a hot spot independently of its size. By monitoring, it is understood the establishment of the

most important fire parameters with a view to obtain relevant information on this phenomenon. Among these parameters are the fire's temperature, the instantaneous area taken by the fire, and the energy intensity.

Both polar and geostationary satellite platforms are used for satellite fire detection and characterization. Geostationary satellites have the high temporal resolution necessary to identify diurnal fire signatures while low earth orbit satellites have the higher spatial resolution necessary to enable detection of smaller fires.

Anyway, each satellite sensor or instrument is constructed with unique and different characteristics so that not all sensors have the appropriate spectral bands to detect fires.

In order to detect a fire from a satellite platform, it is necessary that the sensor have specific spectral bands that work in the spectral range of a surface fire at its maximum energy. This statement has its theoretical explanation in Wien's Displacement Law (1), which states that there is an inverse relationship between the wavelength of the peak emission of a black body and its temperature when expressed as a function of wavelength:

$$\lambda_{\max} (\mu m) = \frac{2898}{T(K)} \quad (\text{eq. 1})$$

If we consider a surface where a wildfire is occurring to be like a black body with temperature ranging from 600 to 1,000 K, Equation 1 tells us that it is best seen in the spectral range of 3 to 5 μm .

In 1981, Matson and Dozier used measurements from this specific spectral range to identify fires for the first time. They succeeded in their goal even because this spectral range has other important property; it is in an atmospheric window where atmospheric attenuation is minimal over the wavelengths used to observe the earth surface.

Since there has never been a satellite dedicated to fire monitoring and measuring, most observations of fires from space are obtained from existing satellites developed for other purposes.

1.3.1 Polar Orbiting Satellite Fire Detection

In this context, the most used fire products have been traditionally based on polar-orbiting sensor data like NOAA-AVHRR, ERS-(A), ATSR(-2), EOS-MODIS and more recently NPP-VIIRS, mainly thanks to their high spatial resolution and acquisition at a global scale.

The NOAA-AVHRR sensor has been the first one to provide satellite hot spot detection (Dozier, 1981), and it has also been a research platform in the development of hot-spot detection algorithms.

The case of the European sensor (A)ATSR (Advanced Along Track Scanning Radiometer) and the World Fire Atlas from 1997 published by the ESA with the ERS-1 and ERS-2 (European Remote Sensing Satellite) satellites data (Arino & Rosaz, 1999) has been used to demonstrate its suitability to fire detection and assessment of vegetation fire emissions.

The appearance of the Moderate Resolution Imaging Spectroradiometer MODIS sensor meant a significant step forward in the observation of forest fires. In fact, from its the beginning the 3.9 μm bands on the MODIS instrument were designed with fire detection in mind. And, at this moment, the MODIS fire product is a consolidated product and a reference for global Earth observation.

The MODIS instrument is on board both the EOS-TERRA (morning pass) and EOS-AQUA (afternoon pass) satellites. Each MODIS instrument provides multiple thermal observations of the Earth in the mid to high latitudes on a daily basis.

The MODIS active fire product detects fires in 1km pixels that are burning at the time of overpass under relatively cloud-free conditions using a contextual algorithm, where thresholds are first applied to the observed middle-infrared and thermal infrared brightness temperature and then false detections are rejected by examining the brightness temperature relative to neighboring pixels (Giglio, L. et al. 2003)

A detected fire does not necessarily mean that the entire area represented by the 1km pixel is on fire. A detection may be the result of intense fire activity covering a small fraction of the pixel area or fire activity occurring over a broader area. Fire detection omission/commission errors may occur due to input data anomalies, limited satellite

observation conditions, and/or potential algorithm limitations.

The Visible Infrared Imaging Radiometer Suite (VIIRS) sensor was launched aboard the Suomi National Polar-orbiting Partnership (NPP) satellite at the end of 2011 and became operative in 2012. It provides similar measurements to MODIS at higher resolution.

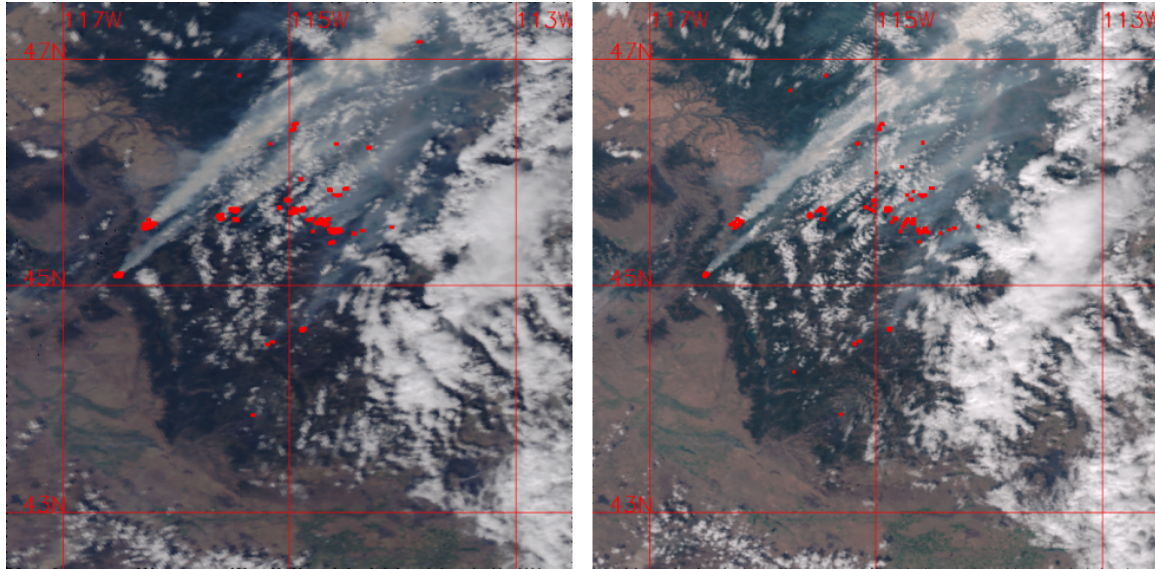


Figure 2: Nearly ten fire complexes were burning in Idaho on September 9th 2014 and both Aqua-MODIS (a) and Suomi-NPP VIIRS (b) detected numerous hot spots. Given the close timing in overpass (Aqua was only 20 minutes behind S-NPP) and similar viewing angle, the agreement in detections is quite good, as evident in the grid plot.

1.3.2 Geostationary Satellite Fire Detection

But the most important limitation of polar satellite systems, with regard to the needs of continuous and in-real-time monitoring of wildfires, is their infrequent overpasses, varying inversely with the spatial resolution of the sensor.

Temporal resolution, on the other hand, is essential for early detection (less time for a fire to burn before an overpass), detection of short-lived fires (a fire may extinguish before an overpass takes place), tracking a fire's evolution over a series of image times, and increasing the opportunities to see a fire under changing cloud conditions.

In this respect only geostationary systems with their inherent high temporal resolution can be helpful; the Spinning Enhanced Visible and Infrared Imager (SEVIRI), on



3ZD REKLAM ve Org. GIDA İNŞ. PAZ. SAN. TİC. LTD. ŞTİ.

board the geostationary Meteosat Second Generation (MSG) satellite, allows for observations over Europe every 15 minutes (or every 5 minutes in the Rapid Scanning Service mode at the expense of coverage).

Despite its coarse spatial resolution (~ 4 km over Southern Europe) recent studies demonstrated that SEVIRI data can be used operationally to assist the detection of fires by improving the reliability in fire announcements (Laneve & Cadau, 2006; Georgiev & Stoyanova, 2013) and allowing real time fire front monitoring in the Mediterranean region. The role of SEVIRI is especially useful as the fires increase in number and size (Sifakis et al. 2011).

Since the launch of Meteosat Second Generation in 2002, a number of studies have used different algorithms to study active fires with SEVIRI observations (e.g. Calle et al., 2009; Amraoui et al., 2010). This has led to certain other routinely generated SEVIRI active fire products being available.

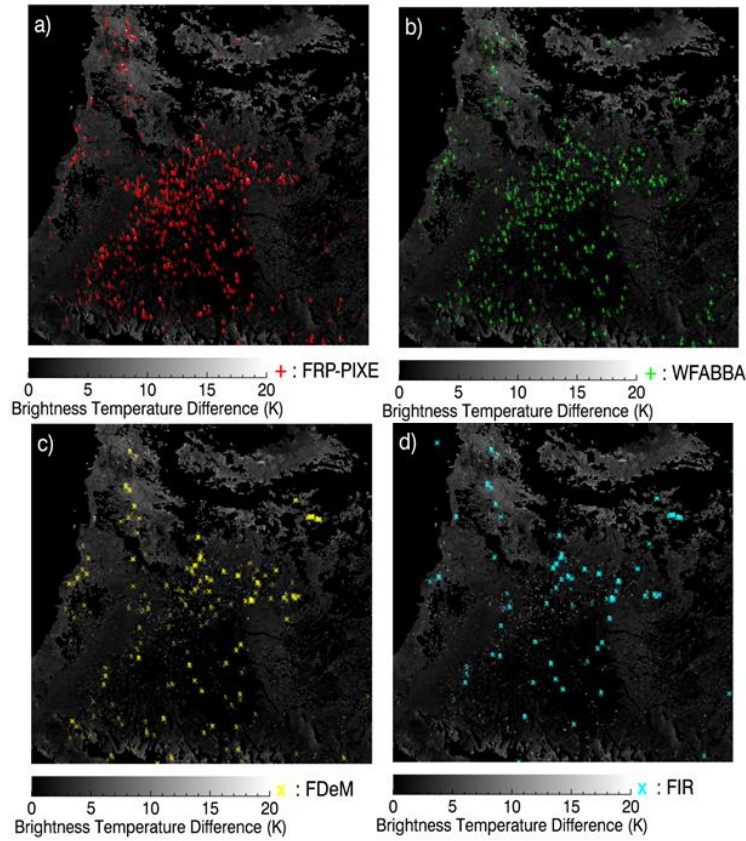


Figure 3: Angola, 21 st August 2014, 13:15 UTC. Example of the active fire pixel detections performed by LSA SAF FRP-PIXEL; WF-ABBA; FDeM; and FIR.

1.4. Burnt Area

Burnt area maps derived from satellite imagery are widely used to investigate the causes and consequences (such as pyrogenic emissions) of vegetation fires. Two products with daily resolution are currently available:

- the L3JRC product (Tansey et al. 2008)
- and the Moderate Resolution Imaging Spectroradiometer Burned Area Product (Roy et al. 2005, 2008).

For both the fire scar detection is based on rapid drops in vegetation-related reflectance of the area affected by the fire burnings.

Major differences have been reported, however, between these fire scar products, mainly on account of overestimation of the burnt area by the L3JRC (Chang and Song 2009, Giglio et al. 2010).

The most widely used is definitely the MODIS one. For this, the mapping of burnt areas is based mainly on the 250 meters bands, although the MODIS bands at 500 meters resolution are also used, as they provide complementary information that is used for improved burnt area discrimination.

This type of satellite imagery allows detailed mapping of fires of about 50 ha or larger. Although only a fraction of the total number of fires is mapped (fires smaller than 40 ha are not mapped). The analysis of historical fire data has determined that the area burnt by wildfires of this size represents in most cases the large majority of the total area burnt. On average, the area burnt by fires of at least 40 ha accounts for about 75% of the total area burnt every year in the Southern Europe (JRC, 2011).

Since the launch of SUOMI-VIIRS, a VIIRS Burned Area product has been developed, that will continue in a consistent manner the 14- year MODIS record of global mapping of fire burned area.

Due to the data and analysis requirements associated with the MODIS science processing algorithms to yield reliable burn scar products, the burn scar data are not available in near real-time. Currently, MODIS burn scar data are compiled by the Active Fire Mapping Program as monthly datasets are typically available approximately 10 days after the beginning of each month. The burn scar data are provided as monthly GeoTiff and KMZ products for the specified geographic regions.

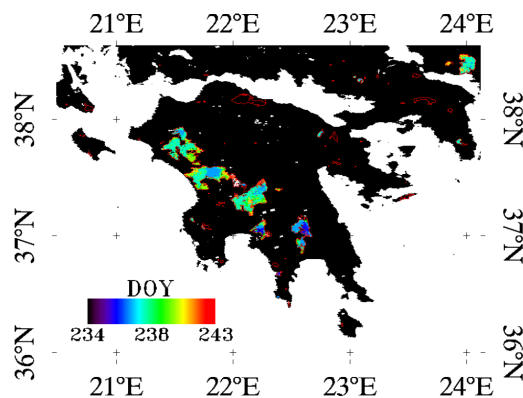


Figure 4: The Peloponnese wildfires as viewed by the MODIS 500m burned area of Roy et al. (2005) collected in August and September 2007 and coloured by day of the year they were detected (DOY). The fires occurred in areas forest, shrublands and olive groves and affected 1847 km².

SEVIRI and MODIS based fire detection and characterization products will be used in this analysis to test the performances of the available most advanced fire detection products over the Turkish territory using historical available ground observations. We will describe their ability to detect the reported fire episodes with respect to their first ground observation.

2. SATELLITE FIRE OBSERVATION FOR THE SELECTED CASE STUDY

The aim of this study is to analyze how satellite observations are able to describe biomass burnings over Turkey. The two most stable geostationary and polar satellite based fire products for the European region are selected in order to describe the 2008 fire season over two provinces of Turkey.

Respectively the The Fire Radiative Power (FRP) product of Land Surface Analysis (LSA) Satellite Application Facilities (SAF) Programme of EUMETSAT based on data from Meteosat Second Generation (MSG) satellites, and the Fire Information for Resource Management System at the land surface of National Aeronautics and Space Administration (NASA) based on MODIS instrument on Aqua/Terra satellites.

Fire observed by both satellite fire products are presented in form of geolocated points and listed with information of the first and last satellite detection.

2.1. Data

SEVIRI LSA SAF

The Spinning Enhanced Visible and Infrared Imager (SEVIRI) onboard the Meteosat Second Generation (MSG) series of satellites acquires observations every 15 min over the Earth's disk centered on West Africa, including in medium-wave infrared (MWIR) and long-wave infrared (LWIR) wavebands. Data collected in these wavebands enables the detection of active fires and this has been exploited for the development of a number of geostationary active fire products based on SEVIRI observations.

One of these is the Meteosat SEVIRI FRP-PIXEL family of products that has been produced operationally since 2008 by the European Organisation for the Exploitation of Meteorological Satellites (EUMETSAT) LSA SAF (<http://landsaf.meteo.pt>).

The LSA SAF FRP-PIXEL product provides information on the spatial location, thermal properties, atmospherically corrected FRP and uncertainty of pixels containing actively burning fires every 15 min over Europe, North and South Africa and part of South America. These information are delivered into two discrete files:

- The FRP-PIXEL “Quality Product” file, a 2-D dataset that provides information on the status of each SEVIRI pixel in the geographic region under study (e.g. whether it is a cloud, water, or land pixel, whether it has been classed as containing an active fire etc; Wooster et al., 2015).
- A smaller “List Product” file that provides detailed information of pixels in which active fires have been detected (e.g. including the pixel MWIR and LWIR brightness temperatures, FRP, FRP uncertainty, latitude and longitude, and some of the metrics derived during algorithm application such as background window size and estimated MWIR band atmospheric transmissivity).

MODIS FIRMS

The Moderate Resolution Imaging Spectroradiometer MODIS instrument is on board both the EOS-TERRA (morning pass) and EOS-AQUA (afternoon pass) satellites. Each MODIS instrument provides multiple thermal observations of the Earth in the mid to high latitudes on a daily basis.

The MODIS Fire Information for Resource Management System (FIRMS) detects fires in 1km pixels that are burning at the time of overpass under relatively cloud-free conditions using a contextual algorithm, where thresholds are first applied to the observed middle–infrared and thermal infrared brightness temperature and then false detections are rejected by examining the brightness temperature relative to neighboring pixels (Giglio, L. et al. 2003).

The relatively high spatial resolution of MODIS' active fire observations (1 km at nadir), and the high saturation temperature of its MWIR channel (500 K), coupled with its better than daily availability from two platforms (the Terra and Aqua satellites), ensure that the MODIS active fire product is the standard against which geostationary active fire products are compared when performing product evaluations. In this study we use near-simultaneously recorded Collection 5 MODIS active fire detections, MOD14 from Terra and MYD14 from Aqua (<https://earthdata.nasa.gov/data/near-real-time-data/firms>).

Case study selection

In 2008 most of the large forest damages in Europe occurred in the Southeastern Mediterranean countries, which were under the influence of extreme weather conditions that facilitated fire ignition and spread. The country that was most heavily damaged was Turkey, where the forest fire danger was high during the period May to October, and especially during the period July to September, which had very high temperatures, very low humidity and effective wind.

According to the annual European Forest Fire Report (JRC, 2013), this was the most intense fire season in Turkey over the last 20 years, hence the most intense fire season since the launch of the satellites described in this study.

In Turkey, the coastline, which starts from Hatay and extends over the Mediterranean and Aegean up to Istanbul, has the highest fire risk.

In the light of this, we decide to perform our analysis over two provinces located in this fire sensitive area, Mugla and Antalya, and during the period June – September 2008.

2.2. Satellite fire observations

SEVIRI and MODIS detection locations for the selected case study are depicted in Figures 5,6,7 and 8 over a map showing the administrative borders at the province

and municipality level. Each detection is grouped according to its relative FRP¹ value. We can notice how MODIS, thanks to its higher spatial resolution, is able to detect many more hot spots with lower FRP than SEVIRI. For example, over the province of Mugla during summer 2008 the MODIS algorithm detected 13 fire pixels with FRP less than 30 MW while the SEVIRI based one did not detect any in this category. On the other hand we can see how the absolute number of detections is much higher for the geostationary-based fire product than for the polar-based one.

A detected fire does not necessarily mean that the entire area represented by the ~4km (SEVIRI) or 1km (MODIS) pixel is on fire. A detection may be the result of intense fire activity covering a small fraction of the pixel area or fire activity occurring over a broader area. Also fire detection omission/commission errors may occur due to input data anomalies, limited satellite observation conditions, and/or potential algorithm limitations.

Depending on the observed fire dynamic, multiple detection of the same fire episode can be reported by the selected fire algorithms. To define a fire episode we aggregate pixel detections on the basis of spatial and temporal closeness. Figures 7 and 10 and Tables 1 and 2 show the fire episode locations and information about the relative first and last detection² plus the number of detections reported for each fire episode.

During summer 2008 SEVIRI LSA SAF and MODIS FIRMS detected respectively 21 and 8 fires over the province of Mugla, 4 of these fires were commonly detected by both fire products, for a total of 25 fires. Over the province of Antalya and during the same period these fire algorithms reported respectively 80 and 16 fires, with two common detections, for a total of 94 fires.

Many hot spots have been observed only once by SEVIRI and MODIS fire products,

¹ Spaceborne sensors, as MODIS and SEVIRI, able to observe the Middle Infrared (MIR) spectral radiance that is coming from the Earth can measure the radiative component of the energy released by open fires (Wooster et al., 2003). Fire Radiative Power (FRP) is a measure of the radiant energy liberated per unit time from burning vegetation via the rapid oxidation of fuel carbon and hydrogen. It has been demonstrated in small-scale experiments that this parameter, is related to the rate at which the fuel biomass is being consumed.

² The time scale for all fire detections has been converted from UTC to local time (LT), that is also more easily linked to the diurnal cycle of the fires.

while there is a small group of them observed continuously several times during one or two days and even one observed during few days, with 1375 and 246 detections respectively for SEVIRI and MODIS.

We can also notice that most of the satellite observed fire occurrences in summer 2008 in these two provinces were in forested areas, that extent over a large part of the studied territories.

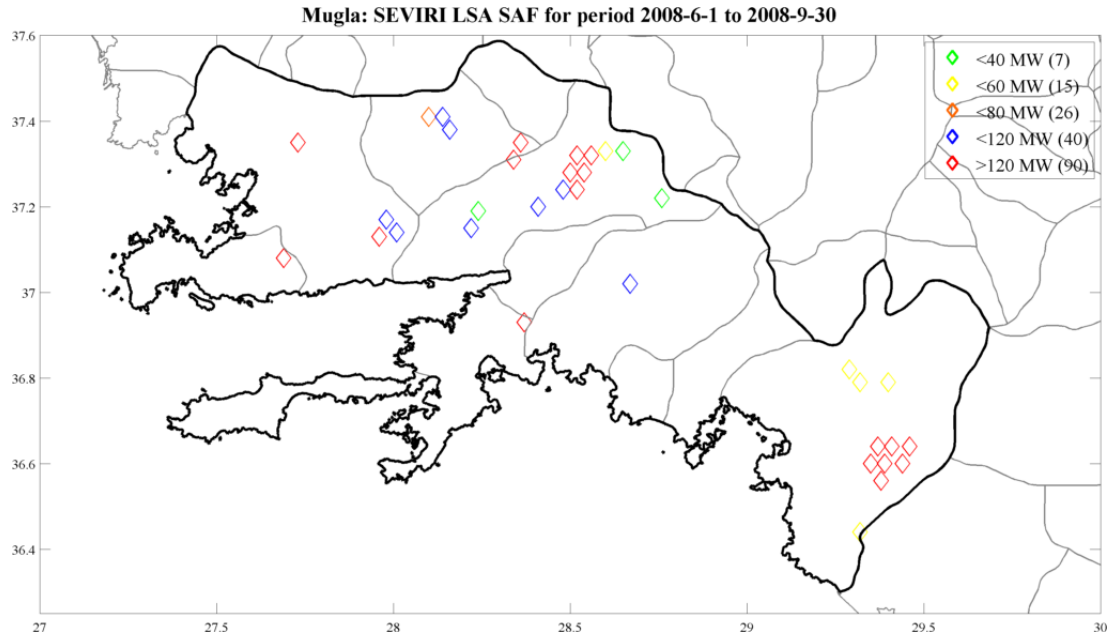


Figure 5. SEVIRI LSA SAF detection locations over the Mugla province during summer 2008

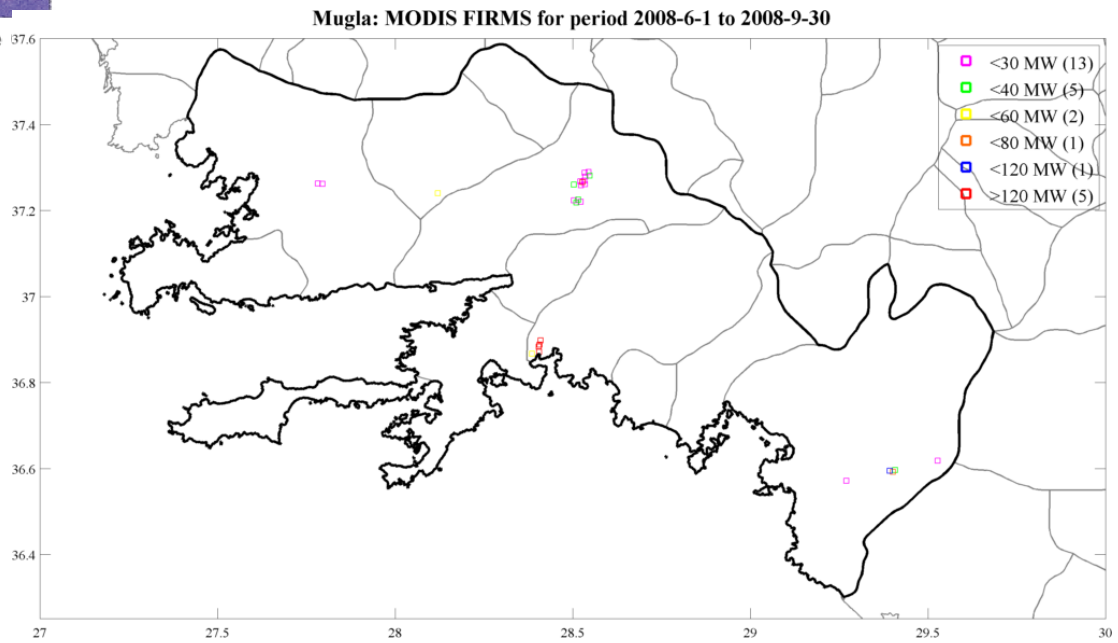


Figure 6. MODIS FIRMS detection locations over the Mugla province during summer 2008

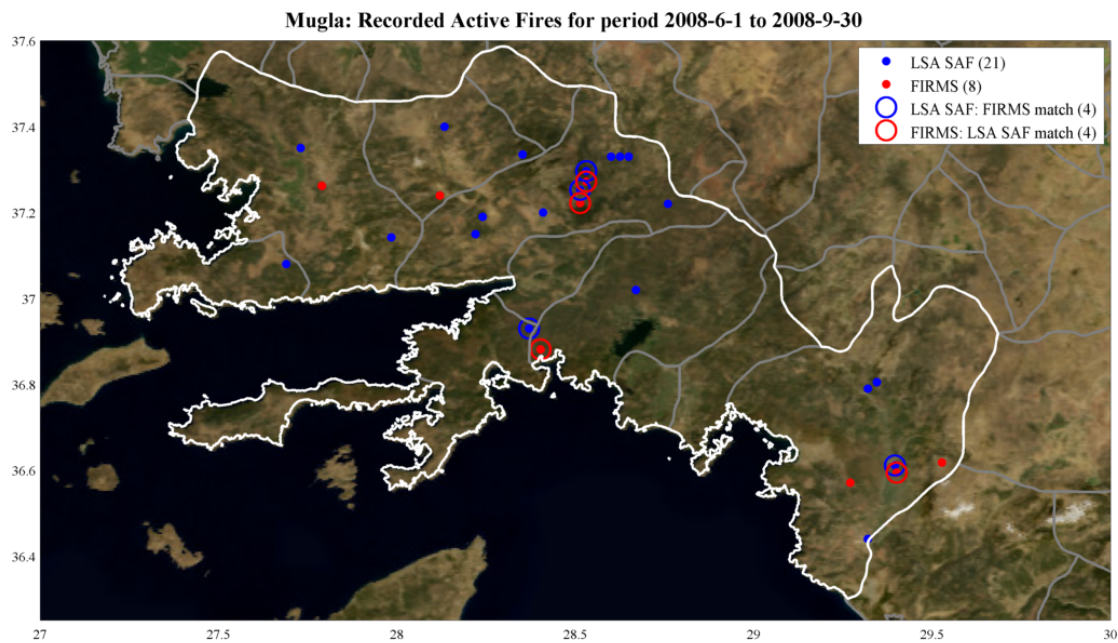


Figure 7. SEVIRI LSA SAF and MODIS FIRMS detected fire locations over the Mugla province during summer 2008, over a MODIS Blue Marble image.

first detection		last detection		location		number of detections	satellite
day	time	day	time	lat	lon		
7-Jun	1925	7-Jun	1925	37.33	28.65	1	MSG-SEVIRI
15-Jun	1940	15-Jun	1940	37.33	28.6	1	MSG-SEVIRI
21-Jun	1210	21-Jun	1225	37.02	28.67	2	MSG-SEVIRI
22-Jun	1910	22-Jun	1910	37.19	28.24	1	MSG-SEVIRI
22-Jun	1925	22-Jun	1925	37.22	28.76	1	MSG-SEVIRI
4-Jul	1407	4-Jul	1407	36.571	29.271	1	EOS-MODIS
5-Jul	1450	5-Jul	1450	37.24	28.12	1	EOS-MODIS
8-Jul	1755	8-Jul	1755	37.35	27.73	1	MSG-SEVIRI
11-Jul	1710	11-Jul	1740	37.08	27.69	3	MSG-SEVIRI
13-Jul	0810	13-Jul	0810	37.33	28.625	2	MSG-SEVIRI
15-Jul	1210	15-Jul	1325	36.93	28.37	5	MSG-SEVIRI
15-Jul	1210	15-Jul	1349	36.882	28.403	5	EOS-MODIS
21-Jul	1840	21-Jul	1840	37.15	28.22	1	MSG-SEVIRI
22-Jul	1216	22-Jul	1216	36.618	29.528	1	EOS-MODIS
26-Jul	1455	26-Jul	1455	37.2	28.41	1	MSG-SEVIRI
26-Jul	1455	26-Jul	1455	37.4	28.133	3	MSG-SEVIRI
26-Jul	1825	26-Jul	1825	37.33	28.6	1	MSG-SEVIRI
1-Aug	1425	1-Aug	1810	36.611	29.396	67	MSG-SEVIRI
1-Aug	1432	1-Aug	1432	36.594	29.401	3	EOS-MODIS
9-Aug	1625	9-Aug	1725	37.335	28.352	8	MSG-SEVIRI
15-Aug	1444	15-Aug	1444	37.263	27.79	2	EOS-MODIS
23-Aug	1855	23-Aug	1940	37.142	27.984	5	MSG-SEVIRI
23-Aug	2320	23-Aug	2320	37.222	28.514	4	EOS-MODIS
23-Aug	2340	23-Aug	2340	37.253	28.513	3	MSG-SEVIRI
25-Aug	1340	25-Aug	2310	37.296	28.531	68	MSG-SEVIRI
25-Aug	1343	25-Aug	2307	37.272	28.531	10	EOS-MODIS
1-Sep	1140	1-Sep	1140	36.79	29.32	1	MSG-SEVIRI
15-Sep	1855	15-Sep	1855	36.805	29.345	2	MSG-SEVIRI
25-Sep	2240	25-Sep	2240	36.44	29.32	1	MSG-SEVIRI

Table 1. Fires detected by SEVIRI LSA SAF (blue) and MODIS FIRMS (red) over the province of Mugla during summer 2008.

Antalya: SEVIRI LSA SAF for period 2008-6-1 to 2008-9-30

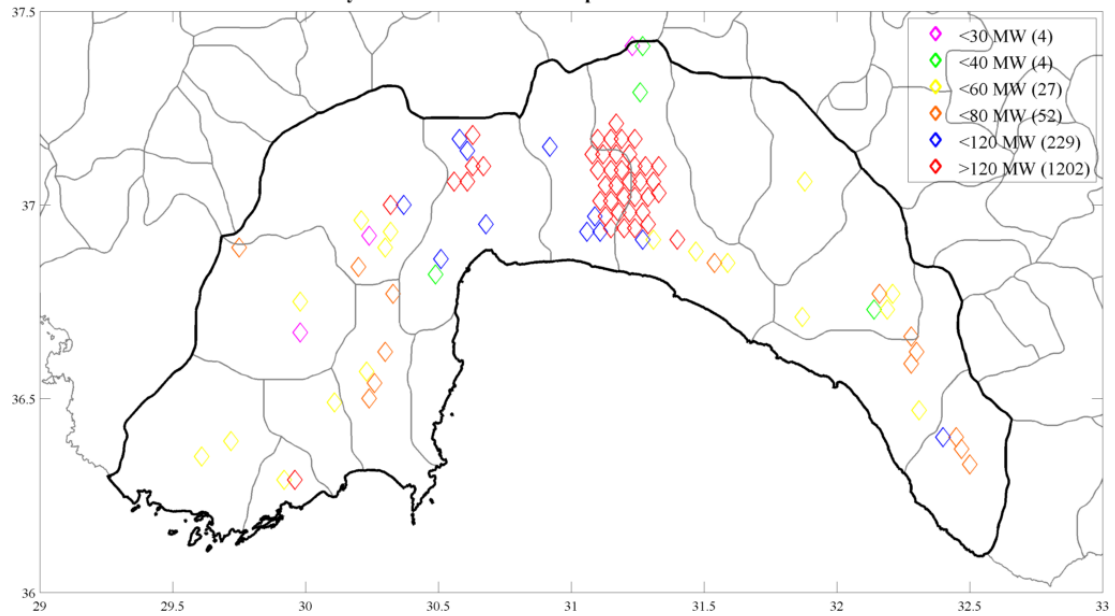


Figure 8. SEVIRI LSA SAF detection locations over the Antalya province during summer 2008.

Antalya: MODIS FIRMS for period 2008-6-1 to 2008-9-30

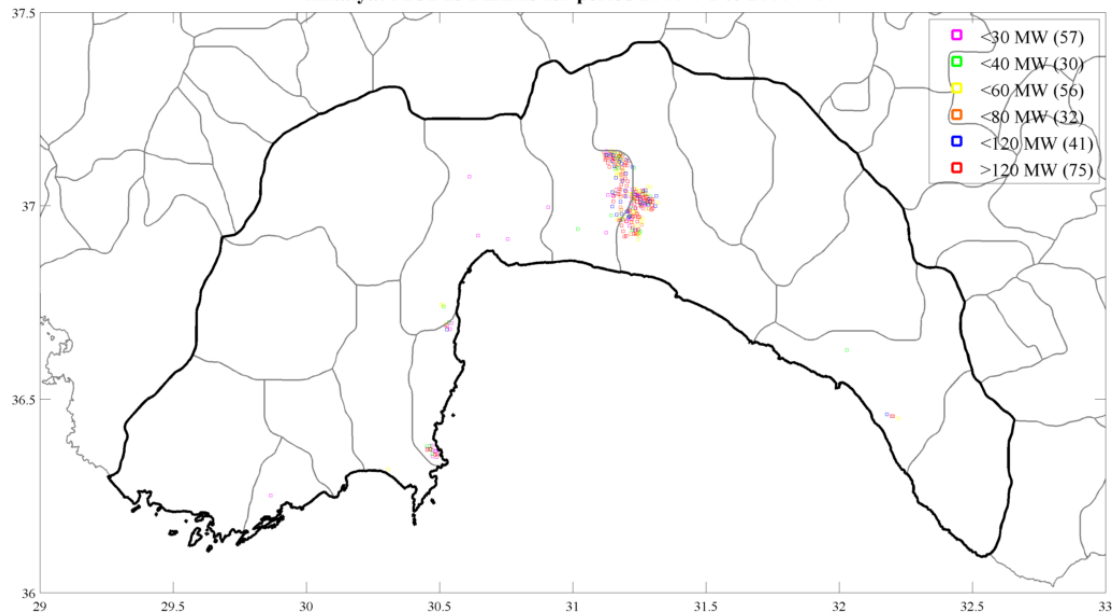


Figure 9. MODIS FIRMS detection locations over the Antalya province during summer 2008

Antalya: Recorded Active Fires for period 2008-6-1 to 2008-9-30

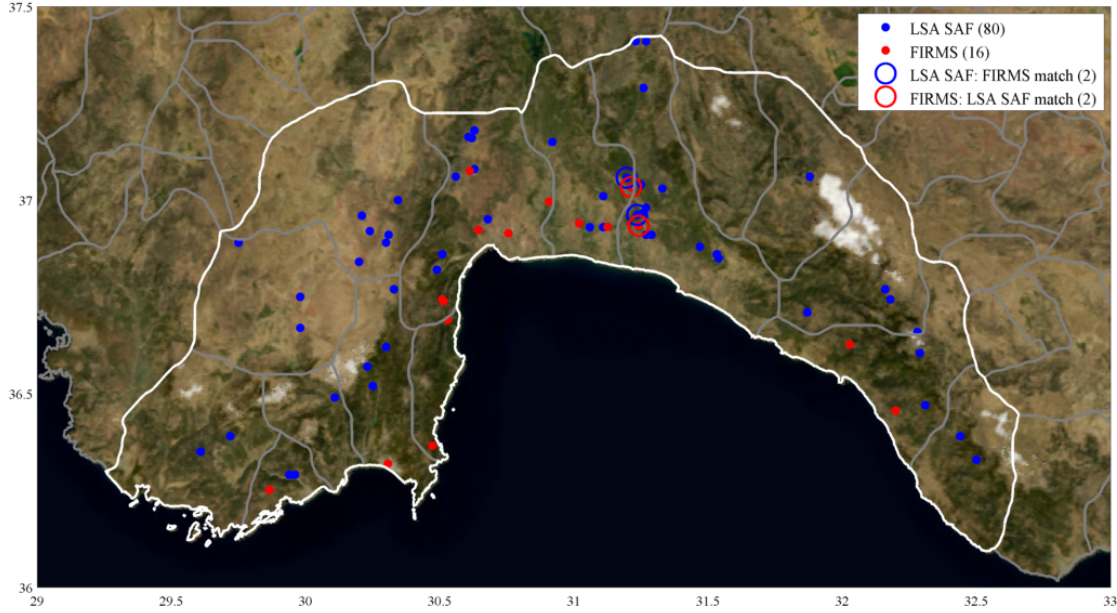


Figure 10. SEVIRI LSA SAF and MODIS FIRMS detected fire locations over the Antalya province during summer 2008, over a MODIS Blue Marble image.

first detection		last detection		location		number of detections	satellite
day	time	day	time	lat	lon		
1-Jun	0925	1-Jun	0925	36.29	29.96	1	MSG-SEVIRI
6-Jun	0610	6-Jun	0610	36.92	30.24	1	MSG-SEVIRI
7-Jun	1825	7-Jun	1825	36.82	30.49	1	MSG-SEVIRI
8-Jun	1925	8-Jun	1925	36.84	30.2	1	MSG-SEVIRI
10-Jun	1940	10-Jun	1940	37.41	31.27	1	MSG-SEVIRI
11-Jun	1401	11-Jun	1401	37.075	30.612	1	EOS-MODIS
12-Jun	1810	12-Jun	1810	36.75	29.98	1	MSG-SEVIRI
15-Jun	1055	15-Jun	1055	37.06	30.56	1	MSG-SEVIRI
18-Jun	1407	20-Jun	1355	36.69	30.53	9	EOS-MODIS
20-Jun	1140	20-Jun	1140	36.86	30.51	1	MSG-SEVIRI
20-Jun	1310	20-Jun	1425	36.962	31.235	22	MSG-SEVIRI
20-Jun	1355	20-Jun	1355	36.933	31.241	4	EOS-MODIS
22-Jun	1040	22-Jun	1040	36.35	29.61	1	MSG-SEVIRI
23-Jun	0022	23-Jun	0022	36.456	32.2	4	EOS-MODIS
26-Jun	1355	26-Jun	1355	37	30.345	2	MSG-SEVIRI
27-Jun	1222	27-Jun	1222	36.996	30.908	1	EOS-MODIS
29-Jun	0655	29-Jun	0655	37.06	31.88	1	MSG-SEVIRI
30-Jun	1055	30-Jun	1140	36.29	29.96	4	MSG-SEVIRI
1-Jul	1158	1-Jul	1158	36.923	30.644	1	EOS-MODIS
2-Jul	1125	2-Jul	1125	36.29	29.96	1	MSG-SEVIRI



3ZD REKLAM ve Org. GIDA İNŞ. PAZ. SAN. TİC. LTD. ŞTİ.

3-Jul	1040	3-Jul	1040	37.18	30.63	1	MSG-SEVIRI
5-Jul	1025	5-Jul	1025	36.29	29.96	1	MSG-SEVIRI
5-Jul	1940	5-Jul	1940	37.41	31.27	1	MSG-SEVIRI
6-Jul	1040	7-Jul	1110	36.29	29.96	2	MSG-SEVIRI
10-Jul	1010	10-Jul	1055	36.95	30.68	2	MSG-SEVIRI
11-Jul	0625	11-Jul	0625	37.06	31.88	1	MSG-SEVIRI
11-Jul	1010	11-Jul	1010	36.96	30.21	1	MSG-SEVIRI
11-Jul	1910	11-Jul	1910	36.39	29.72	1	MSG-SEVIRI
13-Jul	0910	13-Jul	0910	36.52	30.25	2	MSG-SEVIRI
13-Jul	0925	13-Jul	1055	36.29	29.96	3	MSG-SEVIRI
17-Jul	1025	17-Jul	1110	36.29	29.96	3	MSG-SEVIRI
19-Jul	1110	20-Jul	1055	36.29	29.96	5	MSG-SEVIRI
23-Jul	0955	23-Jul	1010	37.18	30.63	2	MSG-SEVIRI
23-Jul	1040	23-Jul	1040	36.91	31.29	2	MSG-SEVIRI
23-Jul	1040	23-Jul	1040	36.93	31.11	1	MSG-SEVIRI
23-Jul	1055	23-Jul	1055	36.85	31.54	1	MSG-SEVIRI
23-Jul	1055	23-Jul	1055	36.93	31.06	1	MSG-SEVIRI
23-Jul	1125	23-Jul	1125	36.86	31.533	3	MSG-SEVIRI
25-Jul	0810	25-Jul	0810	37.03	31.33	1	MSG-SEVIRI
25-Jul	0855	25-Jul	0855	36.71	31.87	1	MSG-SEVIRI
25-Jul	0855	25-Jul	0855	37.01	31.11	1	MSG-SEVIRI
25-Jul	0925	25-Jul	0925	36.98	31.27	1	MSG-SEVIRI
25-Jul	1025	25-Jul	1025	37.15	30.92	1	MSG-SEVIRI
25-Jul	1025	25-Jul	1025	37.18	30.63	1	MSG-SEVIRI
26-Jul	1010	26-Jul	1025	36.71	31.87	2	MSG-SEVIRI
26-Jul	1455	26-Jul	1455	36.66	32.28	1	MSG-SEVIRI
26-Jul	1455	26-Jul	1455	36.77	32.16	1	MSG-SEVIRI
27-Jul	0655	27-Jul	0655	36.33	32.5	1	MSG-SEVIRI
27-Jul	0655	27-Jul	0655	36.77	32.16	1	MSG-SEVIRI
27-Jul	0710	27-Jul	0710	36.39	32.44	3	MSG-SEVIRI
27-Jul	0940	27-Jul	0940	36.29	29.96	1	MSG-SEVIRI
27-Jul	0940	27-Jul	0940	36.47	32.31	1	MSG-SEVIRI
27-Jul	0955	27-Jul	0955	36.29	29.96	1	MSG-SEVIRI
27-Jul	0955	27-Jul	0955	36.47	32.31	1	MSG-SEVIRI
27-Jul	1010	27-Jul	1010	36.29	29.94	2	MSG-SEVIRI
27-Jul	1010	27-Jul	1010	37.16	30.62	2	MSG-SEVIRI
27-Jul	1025	28-Jul	0925	36.29	29.96	3	MSG-SEVIRI
27-Jul	1413	27-Jul	1413	36.94	31.019	1	EOS-MODIS
28-Jul	0925	28-Jul	0925	36.89	30.3	1	MSG-SEVIRI
28-Jul	0955	30-Jul	1010	36.29	29.96	5	MSG-SEVIRI
30-Jul	2010	30-Jul	2010	36.89	29.75	1	MSG-SEVIRI

31-Jul	1225	31-Jul	1240	37.08	30.63	4	MSG-SEVIRI
31-Jul	1349	31-Jul	1349	36.627	32.029	1	EOS-MODIS
31-Jul	1610	4-Aug	1710	37.058	31.197	1375	MSG-SEVIRI
31-Jul	2310	4-Aug	0009	37.034	31.213	246	EOS-MODIS
31-Jul	2313	1-Aug	0028	36.743	30.51	2	EOS-MODIS
1-Aug	0029	1-Aug	0029	36.319	30.307	1	EOS-MODIS
1-Aug	1115	1-Aug	1115	36.739	30.515	1	EOS-MODIS
2-Aug	2301	5-Aug	0004	36.366	30.473	16	EOS-MODIS
3-Aug	1225	3-Aug	1225	36.29	29.96	1	MSG-SEVIRI
9-Aug	1040	9-Aug	1110	36.29	29.96	2	MSG-SEVIRI
10-Aug	0655	10-Aug	0655	36.67	29.98	1	MSG-SEVIRI
12-Aug	1110	12-Aug	1110	36.29	29.96	1	MSG-SEVIRI
17-Aug	0655	17-Aug	0655	36.743	32.18	3	MSG-SEVIRI
18-Aug	1155	18-Aug	1155	36.91	31.27	1	MSG-SEVIRI
18-Aug	1155	19-Aug	1055	37.04	31.25	2	MSG-SEVIRI
22-Aug	0640	22-Aug	0640	36.605	32.29	2	MSG-SEVIRI
31-Aug	1225	31-Aug	1225	37.18	30.63	1	MSG-SEVIRI
1-Sep	1025	1-Sep	1025	36.88	31.47	1	MSG-SEVIRI
2-Sep	0725	2-Sep	0725	36.57	30.23	1	MSG-SEVIRI
2-Sep	0725	2-Sep	0725	36.77	30.33	1	MSG-SEVIRI
3-Sep	1125	3-Sep	1125	36.965	31.255	2	MSG-SEVIRI
3-Sep	1158	3-Sep	1158	36.914	30.756	1	EOS-MODIS
4-Sep	1055	4-Sep	1055	36.29	29.96	1	MSG-SEVIRI
5-Sep	1040	5-Sep	1110	36.95	30.68	2	MSG-SEVIRI
5-Sep	1125	5-Sep	1125	36.29	29.96	1	MSG-SEVIRI
5-Sep	1125	5-Sep	1125	36.91	31.27	1	MSG-SEVIRI
8-Sep	1040	8-Sep	1040	36.91	30.31	2	MSG-SEVIRI
9-Sep	1255	9-Sep	1255	36.29	29.96	1	MSG-SEVIRI
9-Sep	1255	9-Sep	1255	37.163	30.607	3	MSG-SEVIRI
10-Sep	1825	10-Sep	1825	37.29	31.26	1	MSG-SEVIRI
14-Sep	1139	14-Sep	1139	36.931	31.126	1	EOS-MODIS
17-Sep	1349	17-Sep	1349	36.251	29.866	1	EOS-MODIS
18-Sep	1910	18-Sep	1910	36.49	30.11	1	MSG-SEVIRI
18-Sep	2225	18-Sep	2225	37.41	31.23	1	MSG-SEVIRI
19-Sep	2025	19-Sep	2025	36.62	30.3	1	MSG-SEVIRI

Table 2. Fires detected by SEVIRI LSA SAF (blue) and MODIS FIRMS (red) over the province of Antalya during summer 2008.

3. PERFORMANCE ANALYSIS

3.1 Ground fire reports

The official fire reports include the following information associated with each of the recorded fires:

- Village near by the event
- Start time
- Total surface area burned

The major limitation of this dataset is the absence of the exact geolocation and the duration of the observed fire episodes.

Also, they do not include a record of cloud cover. The presence of clouds over a fire can make fire detection impossible from a satellite platform, so it is important to be able to evaluate cloud cover over each fire site when the fires were active.

3.2 How close a fire should be in time and space

We need to determine when the satellite fire products used in this study are detecting the same fire as reported by Ministry of Forestry workers to effectively analyze the correspondence between the satellite derived fire product and ground truth.

We consider a ground reported fire collocated with a satellite observation within a spatial window of 20 km and temporal window of minus 6 hours before and plus 48 hours after the reported start times.

These match distance criteria are reasonable if we consider the given spatial resolution at Antalya latitudes (4.5 km sampling size), SEVIRI geolocation accuracy³, and possible uncertainties in ground truth reporting (furthermore the distance from the near by village is probably different for each episode).

³ The geolocation accuracy for SEVIRI is better than 3 km at nadir and better than 0.75km within a 16 by 16 pixel environment. The relative image-to-image collocation accuracy yields a root mean square error (RMSE) of 1.2km (Schmetz et al., 2002).

3.3 Sensitivity analysis

Figure 11, 12, and 13 can give us the very first information of the performance of selected satellite product performances on the chosen case test with the criteria defined above.

LSA SAF (SEVIRI) observed 16 out of the 124 fires reported in the province of Antalya during the summer 2008, while FIRMS (MODIS) detected 12 of them. The two products combined observed a total of 26 episodes.

Given the location of a fire, the size of each fire is another very important piece of information.

We sorted the fires by surface area burned into the following five categories in order to provide a simple visualization of this information:

1. Very small: < 0.1 ha
2. Small: < 1 ha
3. Medium: < 10 ha
4. Large: <100 ha
5. Very large: > 100 ha

Figure 14 shows the geographical distribution of the fire occurrence by size.

Fire size analysis is important because the performances of a fire satellite technique are correlated with the size of the fires.

Figure 14 and 15 respectively show the geolocation of the reported fires and the reported fires collocated with a satellite observation, sorted by size. LSA SAF and FIRMS combined observed:

- ~16% of the CFS fires smaller than 0.1 ha
- ~12% and 4% of the CFS fires smaller 1 ha
- ~18 and 7% of the CFS fires smaller 10 ha
- ~63% and 24% of the CFS fires smaller 100 ha
- ~83% and 74% of the CFS fires larger than 100 ha

The study in California by Koltunov et al (2012) limited the analysis to wildfires with final size exceeding 2 ha, assuming that it is not reasonable to expect detection of

wildfires from geostationary satellites that did not burn more than 2 ha over their lifetime.

For our case study, official reports with a total burned area larger than 2 ha are 23 out of 124 total.

LSA SAF and FIRMS were able to detect respectively 6 and 11 of them

Figure 16, and 17 show the spatial distribution of the detected fires sorted by size together with the collocated satellite detections sorted by estimated Fire Radiative Power. Combined, the LSA SAF and FIRMS products detected 13 out of 23 fires in this category.

A further step in this analysis would be to determine whether the 10 fires that went undetected were effectively observable with the used satellite techniques. This basically means to investigate the presence of cloud covers over them during the period of their activity.

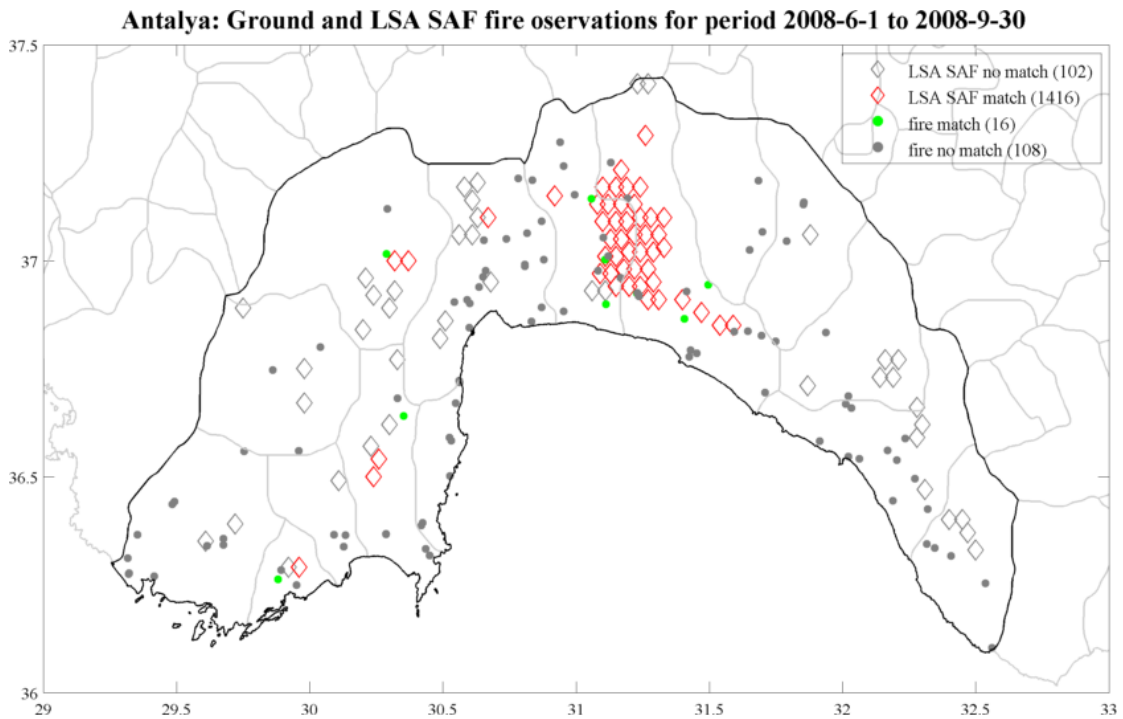


Figure 11. Ground recorded fires with and without a match with LSA SAF (SEVIRI) fire pixels.

Antalya: Ground and FIRMS fire observations for period 2008-6-1 to 2008-9-30

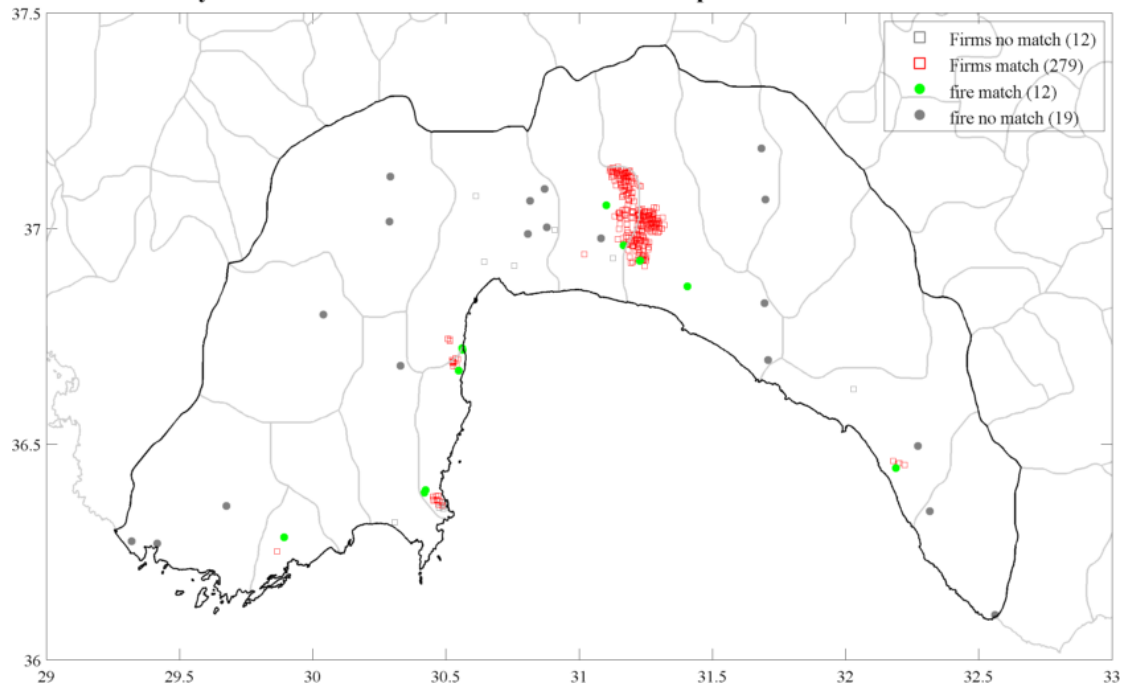


Figure 12. Ground recorded fires with and without a match with FIRMS (MODIS) fire pixels.

Antalya: ground reported fires for period 2008-6-1 to 2008-9-30

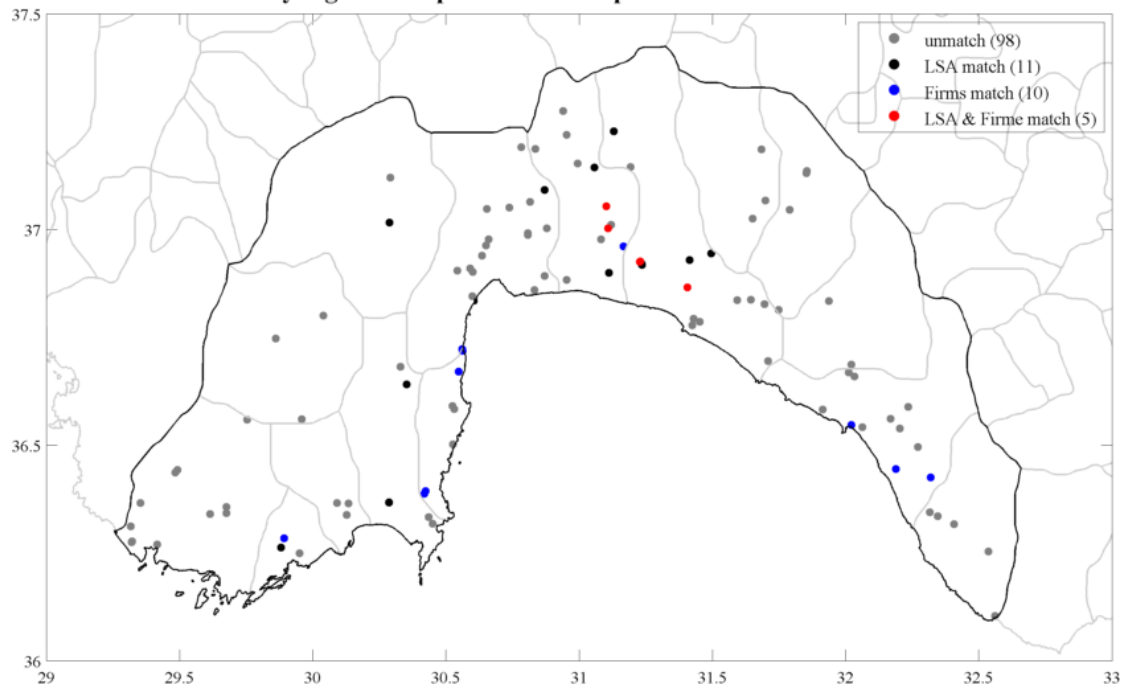


Figure 13. Ground recorded fires without and with a match with LSA SAF (SEVIRI), FIRMS (MODIS) fire pixels, and with the two products combined.

Antalya: ground reported fires for period 2008-6-1 to 2008-9-30

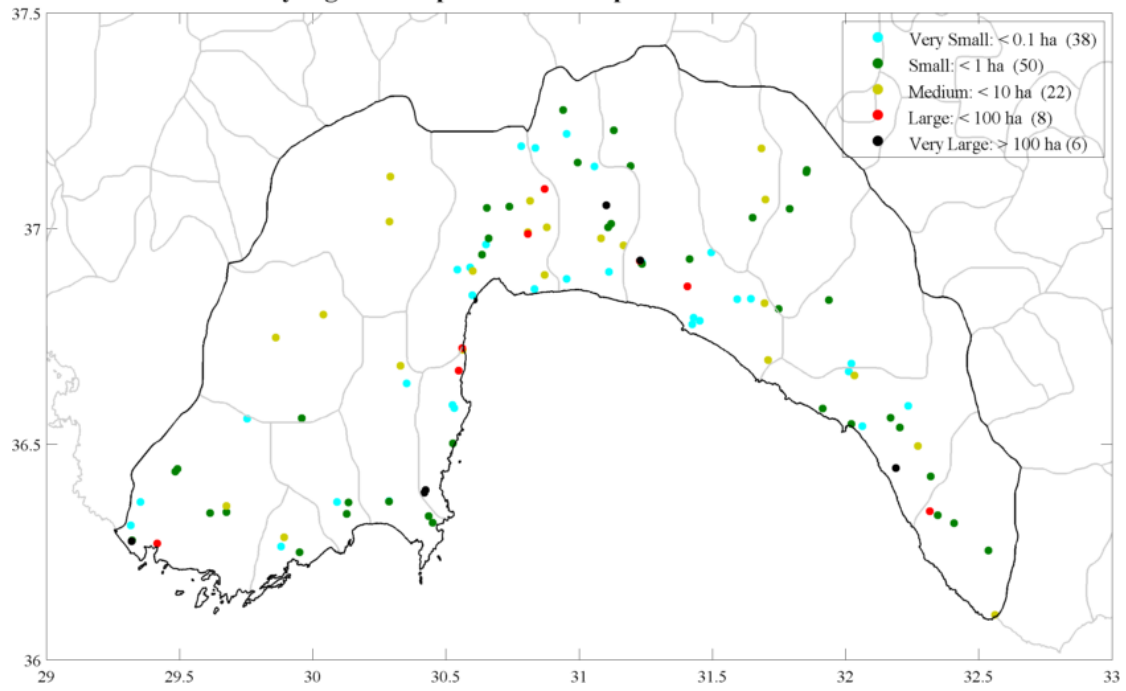


Figure 14. Ground recorded fires sorted by size.

Antalya: satellite observed ground reported fires for period 2008-6-1 to 2008-9-30

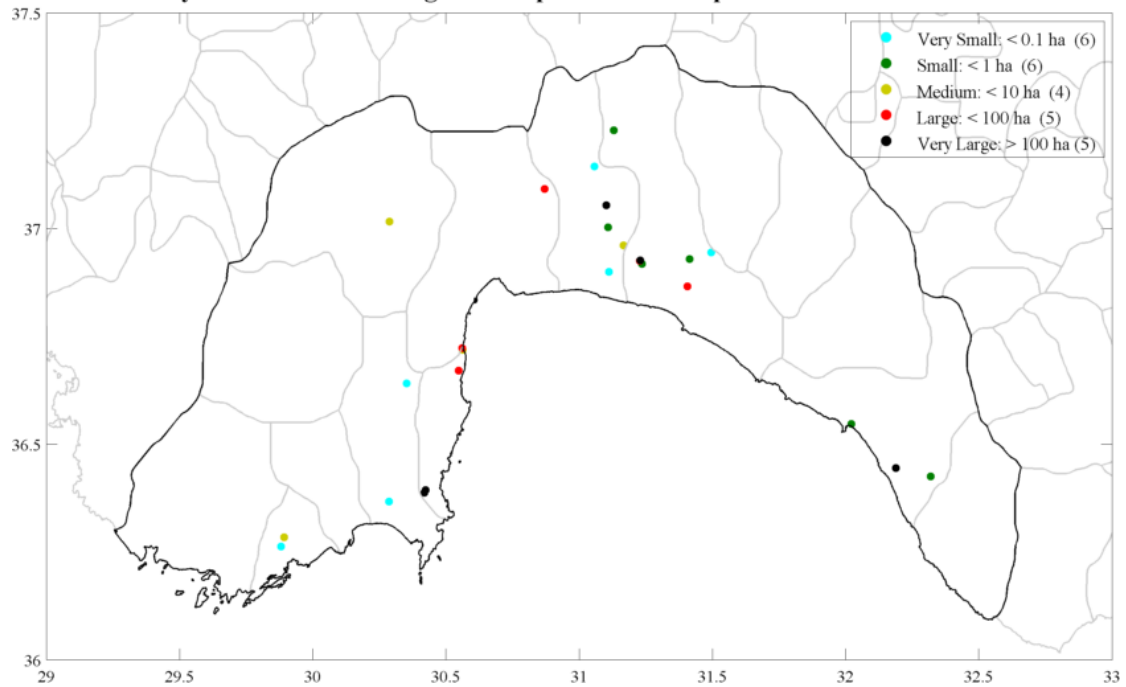


Figure 15. Ground recorded fires, sorted by size, with a match with LSA SAF (SEVIRI) and FIRMS (MODIS) fire pixels.

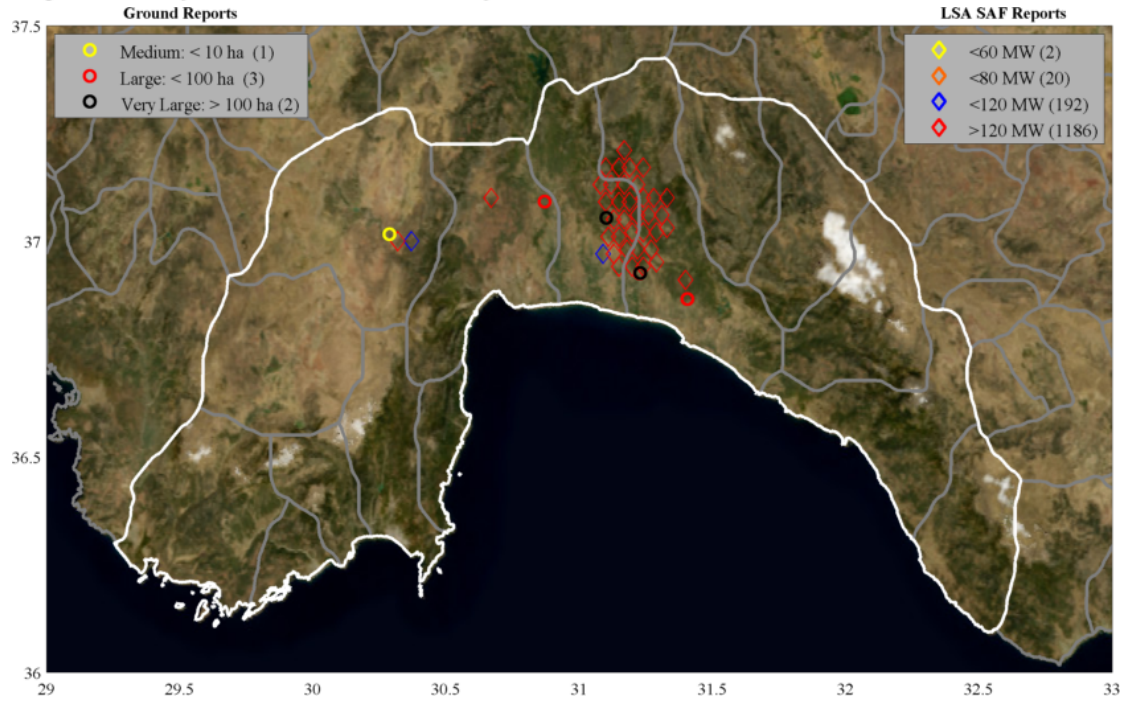


Figure 16. Co-located Ground and LSA SAF (SEVIRI) fire reports over a MODIS Blue Marble image. Ground records are sorted by size, while LSA SAF (SEVIRI) fire pixels are sorted by estimated FRP.

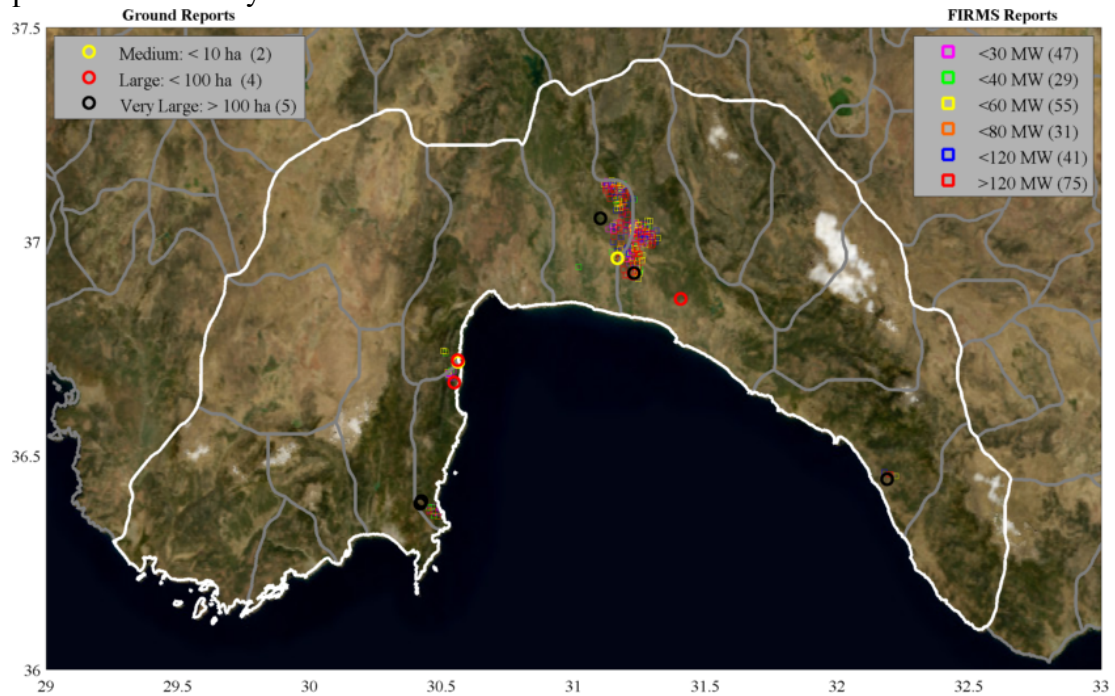


Figure 17. Co-located Ground and LSA SAF (SEVIRI) fire reports over a MODIS Blue Marble image. Ground records are sorted by size, while FIRMS (MODIS) fire pixels are sorted by estimated FRP.

4. Results

Figure 18 shows the spatial distribution of the ground reported fires with final size exceeding 2 ha, together with information of the ones collocated in space and time with the criteria described above, with the selected satellite fire products.

Table 3 provides the burned area and start time characteristics of these fires as reported by the Forest Fire Brigades and the corresponding LSA SAF and FIRMS first detection, including the reason of missed detection based on the visualization of LSA SAF “Quality Product”.

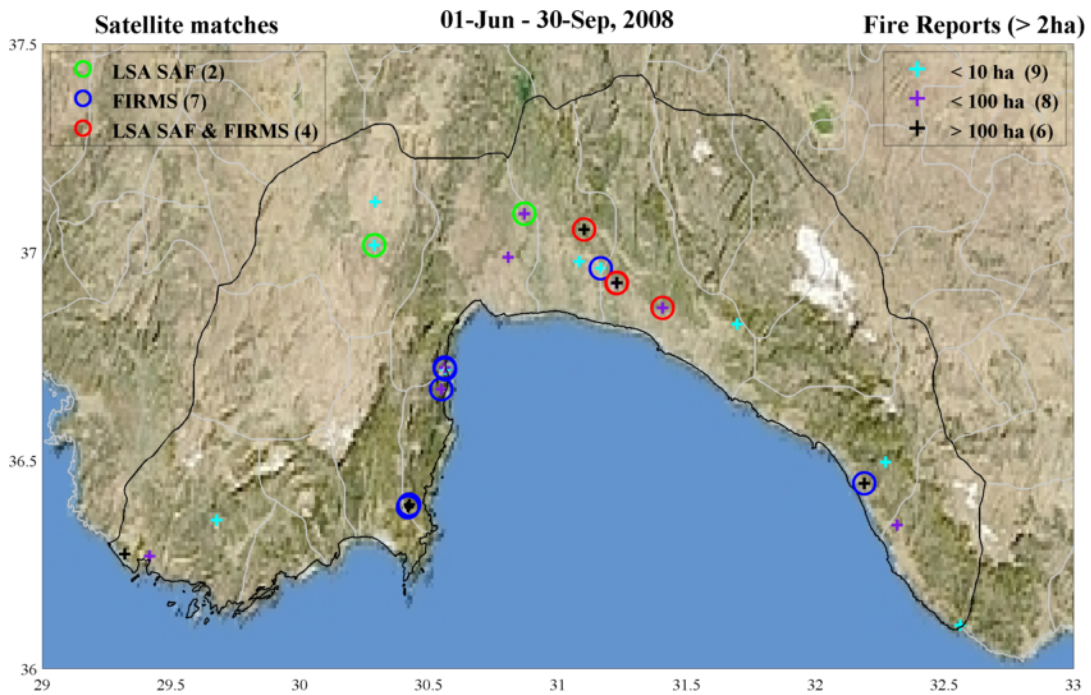


Figure 18. Ground recorded fires (with final burned area exceeding 2 ha), sorted by size, with and without a match with LSA SAF (SEVIRI), FIRMS (MODIS) fire pixels or both.

ID	Ministry of Forestry				LSA SAF-SEVIRI		FIRMS-MODIS	
	Burned Area (ha)	Location	Start day	Start time	day	time	day	time
1	10299.5	Taşagil Belediyesi	31-Jul	12:30	31-Jul	16:15	31-Jul	23:15
2	5688	Akbaş Köyü	31-Jul	16:15	31-Jul	16:15	31-Jul	23:15
3	295	Yazır Köyü	2-Aug	16:05	coast line		2-Aug	23:15
4	210	Patara	11-Jul	17:20	cloud			
5	208	Yazır Köyü	2-Aug	17:00	coast line		2-Aug	23:15
6	114	Aliefendi Köyü	23-Jun	00:55	coast line		23-Jun	03:30
7	50	Göynük Bld.	18-Jun	13:00	coast line		18-Jun	14:15
8	43	şişeler Köyü	3-Aug	14:25	3-Aug	14:45		
9	38	Tasagil	20-Jun	12:45	20-Jun	13:15	20-Jun	14:00
10	26	Güloluk Köyü	29-Jul	15:00	31-Jul	12:30		
11	21.0	Gelemiş Kalkan	18-Sep	14:45	coast line/cloud			
12	20	Fettahlı Köyü	20-Jun	14:10	cloud			
13	15	Beldibi Belediyesi	31-Jul	17:30	coast line		31-Jul	23:15
14	12	Karalar Köyü	31-Jul	05:50	coast line			
15	7.9	Yeşilyurt Köyü	13-Jul	15:20	cloud edge			
16	7	Yazır Köyü	26-Jun	13:45	26-Jun	14:00		
17	4	Tırlar Köyü	11-Jun	12:00	cloud			
18	4	Ahmetler Köyü	3-Sep	12:30	cloud edge/coast line			
19	3	Beldibi Belediyesi	1-Aug	01:00	coast line		31-Jul	23:15
20	2.9	Sarıbalı Köyü	27-Jul	14:25	coast line/sun glint		27-Jul	14:15
21	2.7	Yakacık Köyü	31-Aug	12:15	coast line			
22	2.5	Akörü	5-Jun	11:00	cloud edge			
23	2.5	Küçükköy Belediyesi	23-Jun	14:35	missed detection			

Table 3. On the left side, ground burned area (ha), location and start time (local time) of the fires in Fig, 18. On the right side, corresponding LSA SAF and FIRMS first detection and reason of missed detection based on the visualization of LSA SAF Quality flag.

4.1. Impact of Clouds

As mentioned before, LSA SAF FRP-PIXEL product, together with a list of the detected fires for each SEVIRI acquisition, includes a “Quality Flag Product File”, a 2-D dataset that provides information on the status of each SEVIRI pixel in the geographic region under study.

By visualizing the Quality Product over each fire location at its ground reported start time, we discovered that, out of the 10 fires undetected by satellite, 9 were located in pixels classified as cloud or cloud edges or in pixels surrounded by pixels with these flags.

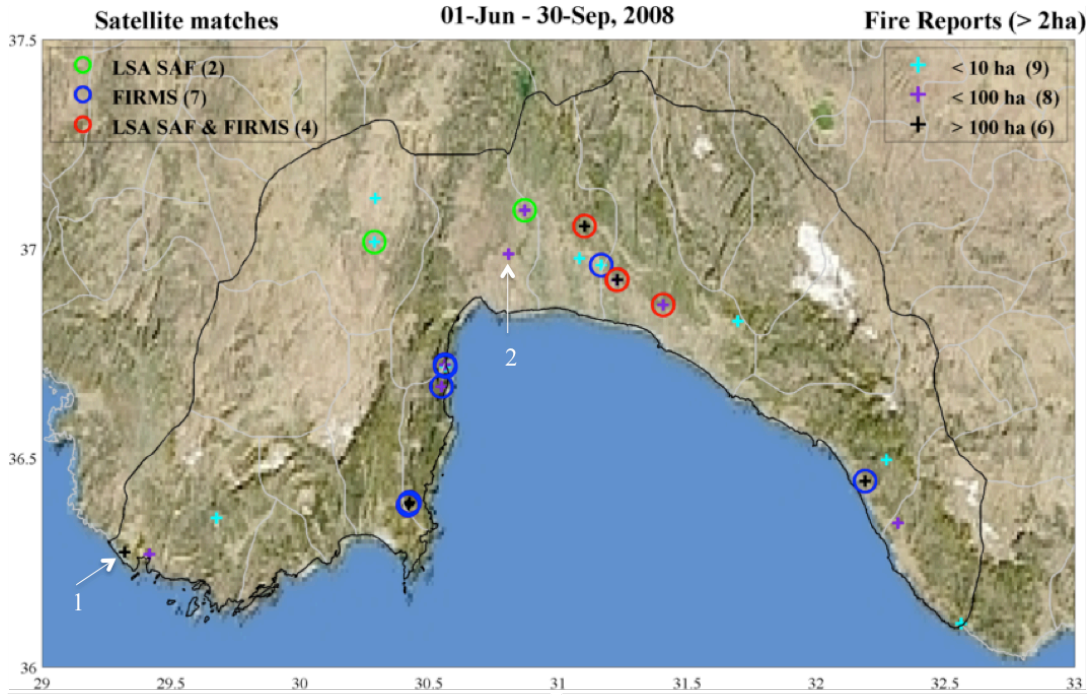
2 of them are located in or nearby pixels classified as cloud edges but that in reality are coast line pixels that are classified in the same way and than excluded from the further steps of the detection chain. This is the same reason way few large fires are



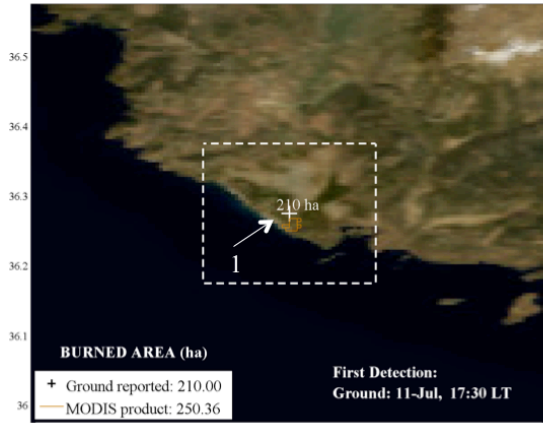
3ZD REKLAM ve Org. GIDA İNŞ. PAZ. SAN. TİC. LTD. ŞTİ.

observed only by FIRMS, and a limitation of the LSA SAF product that should be addressed to the authors of this algorithm. Only one, the smallest of the 23 events reported in Table 3, went undetected in condition of clear sky at its start time.

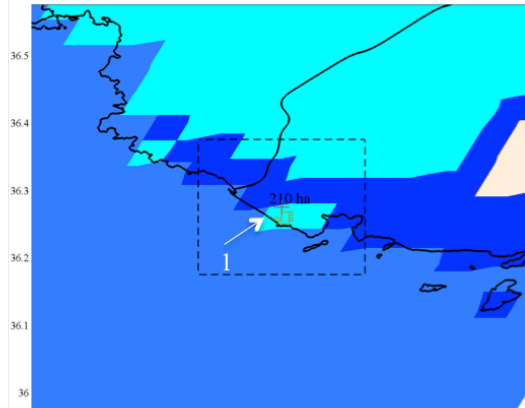
Figure 19 shows two examples of large fires undetected because of cloud covers. It is interesting to notice that the MODIS Burned Area product reported the first of the two fire episodes described in this figure. In fact this product detects the burn scars over the area affected by the fire at the end of combustion process.



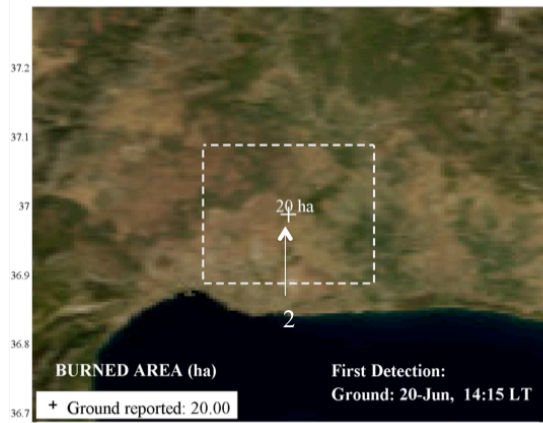
11-Jul - 14-Jul, 2008



Quality Flag: 11-Jul, 17:30 LT



20-Jun - 23-Jun, 2008



Quality Flag: 20-Jun, 14:15 LT

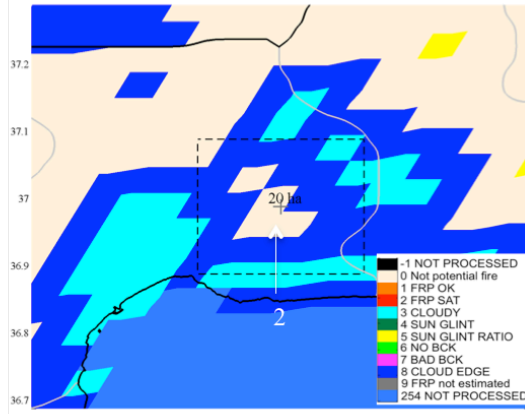


Figure 19. Large panel, same as Fig 18. In the small panels, examples of large fires not observable from satellite because of cloud cover. On the left side, information of the ground recorded and MODIS based (when available) burned area is included, together with ground reported initial time of the selected fire episodes. On the right side the selected fires are located over LSA SAF Quality Flag map, showing cloud-flagged pixels in the area affected by the fire at the time it was first detected by the Forest Fire Brigades. A 0.1x0.1-degree dashed box surrounding the municipality where the fire was detected is also depicted.

4.2. Timely detection

3 out of the 13 matching events were detected from satellite in less than 30 min from the first ground report. Figure 20 shows some of the timely detected fires.

This is a good result if we consider that the study area is one of most touristic of Turkey and during the summer time is more densely populated. In the mobile phone era, in densely populated area, fires are normally reported shortly after they start. Therefore, only for a small fraction of wildfires can satellite observation provide the earliest alarm for this region.

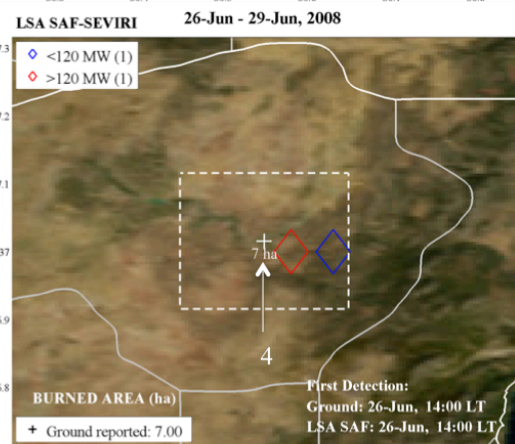
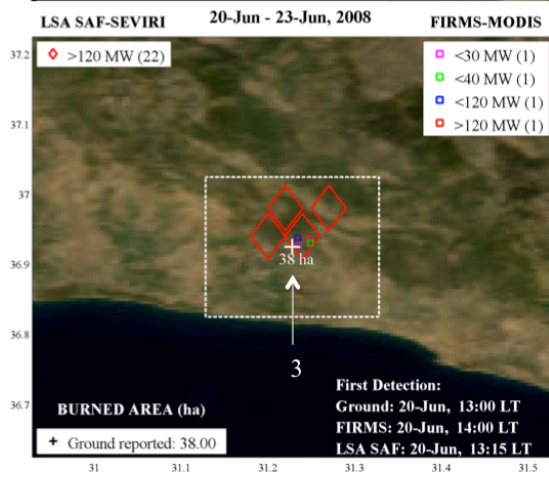
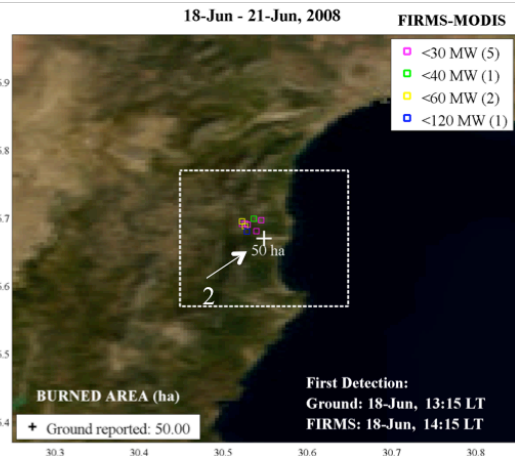
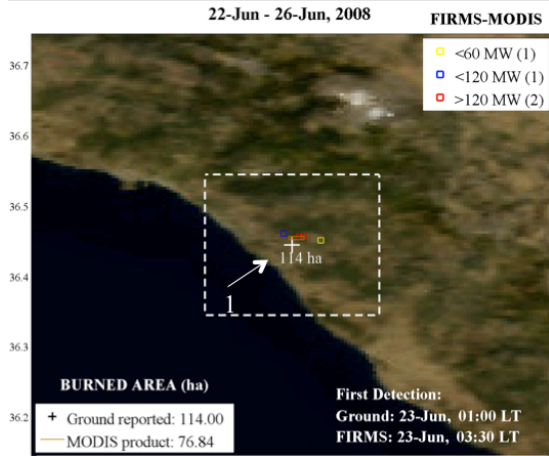
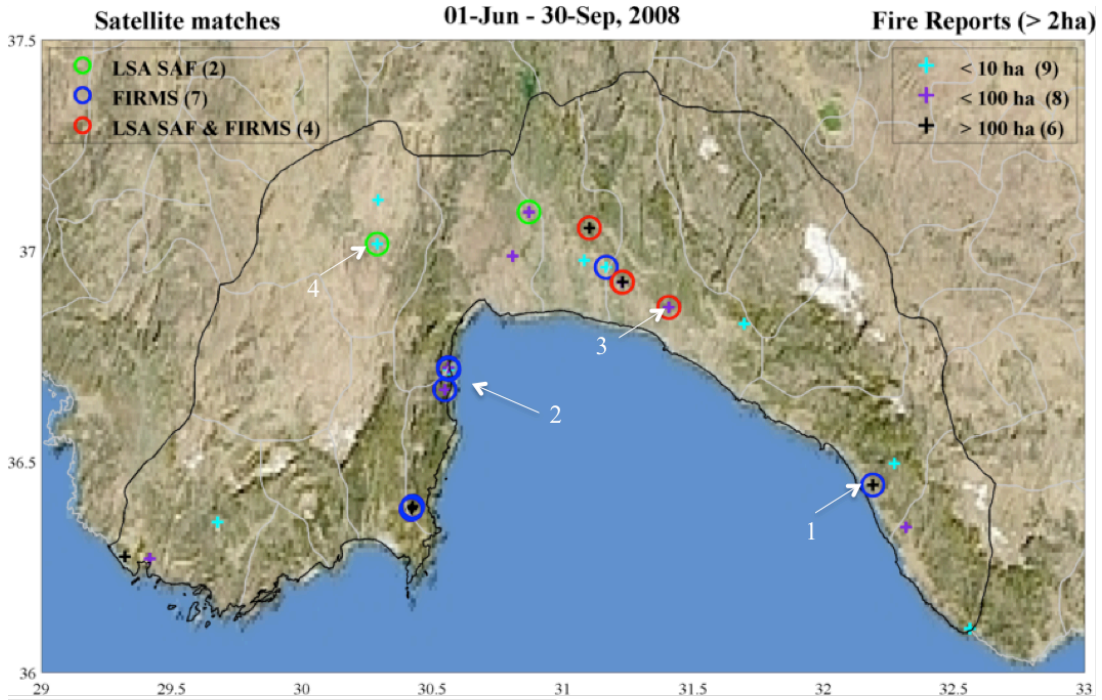


Figure 20. Large panel, same as Fig 18. In the small panels, some ground reported fires, timely detected by the FIRMS-MODIS and LSA SAF-SEVIRI. For each selected fire the corresponding FIRMS and LSA SAF fire pixels sorted by estimated FRP are depicted. Also information of the ground recorded and MODIS based (when available) burned area is included. Ground and satellite first detection is also included on the right bottom part of each panel. A 0.1x0.1-degree dashed box surrounding the municipality where the fire was detected is also depicted.

4.3. Fire monitoring

Figure 21 shows how the selected satellite fire products can describe the largest of the 23 selected fires, recorded in the municipalities of Taşağıl and Akbaş. SEVIRI captured biomass-burning activities from their beginning, as confirmed by ground reported observations, in the early afternoon of the 31 July and monitored the entire lifetime of the fire till the end on 5 August 2008. This fire was an extreme event in terms of energy output.

In Fig. 21c the estimated FRPs, based on SEVIRI and MODIS observations, over the area affected by this event between 31 July and 5 August 2008, are depicted. (The timescale for all the results is in local time (LT) which is more easily linked to the diurnal cycle of the fires.). We notice that the first part of the event (from 31 July to 3 August 2008) was particularly intense, reaching FRP values of 8000 MW (according to LSA SAF FRP-pixel product). MODIS observations, when available, show greater consistency with the LSA SAF product. But, due to its dependence on the scheduled day overpass of EOS AQUA and TERRA, this instrument could not observe the two most intense moments of the fire activity, both in the afternoon of 1 and 2 August 2008.

The graph reveals the pronounced diurnal fire cycle driven by day/night differences in atmospheric humidity, temperature and wind. However, during the second day of the fire, the nocturnal activity was also very strong.

In Fig. 22 the second largest fire of our list is described in a similar fashion. But in this case the SEVIRI based fire product that describes the fire is not LSA SAF but WF ABBA, other geostationary fire detection algorithm described in the first report.

In fact, we noticed that this fire went undetected by LSA SAF because located over pixels reported as “cloud edge” by the Quality Flag map, but they actually belong to coastline pixels that in WF ABBA are normally processed, providing a correct timely detection (within 15 minutes) and monitoring of this large biomass burning.

Together with FRP information, WF ABBA can also provide “Instantaneous Fire Size” and “Temperature”. In Fig. 23 we can visualize this information for the same episode described above.

From Fig. 23a we can observe that this fire was detected for the first time from WF ABBA on August 2 at 16:30 within 1 SEVIRI pixel and with an estimated size of ~2ha (15 times smaller than a SEVIRI pixel at this latitude (~ 3000 ha)). And It was redetected at 17:15 of the same day inside two SEVIRI pixels with a size of ~20 ha. We can also notice that this algorithm is able to detected this fire even when its instantaneous size is smaller then 1 ha.

At the time of its first detection its temperature was estimated in 681 K and it reached a maximum of 1575 K at 23:30 of August 2 (Fig. 6b), with a size of 7.35 ha. At the time of its maximum extension (17:15) its temperature was 953 K.

These pictures show how satellite observations make it possible to quickly locate and monitor large burning areas providing a synoptic picture of the disaster that may support the authorities in the engagement of the appropriate human and technical resources. In some cases, concerning mountainous and inaccessible regions, SEVIRI data are luckily to provide us with the first announcement of fire occurrence in the area.

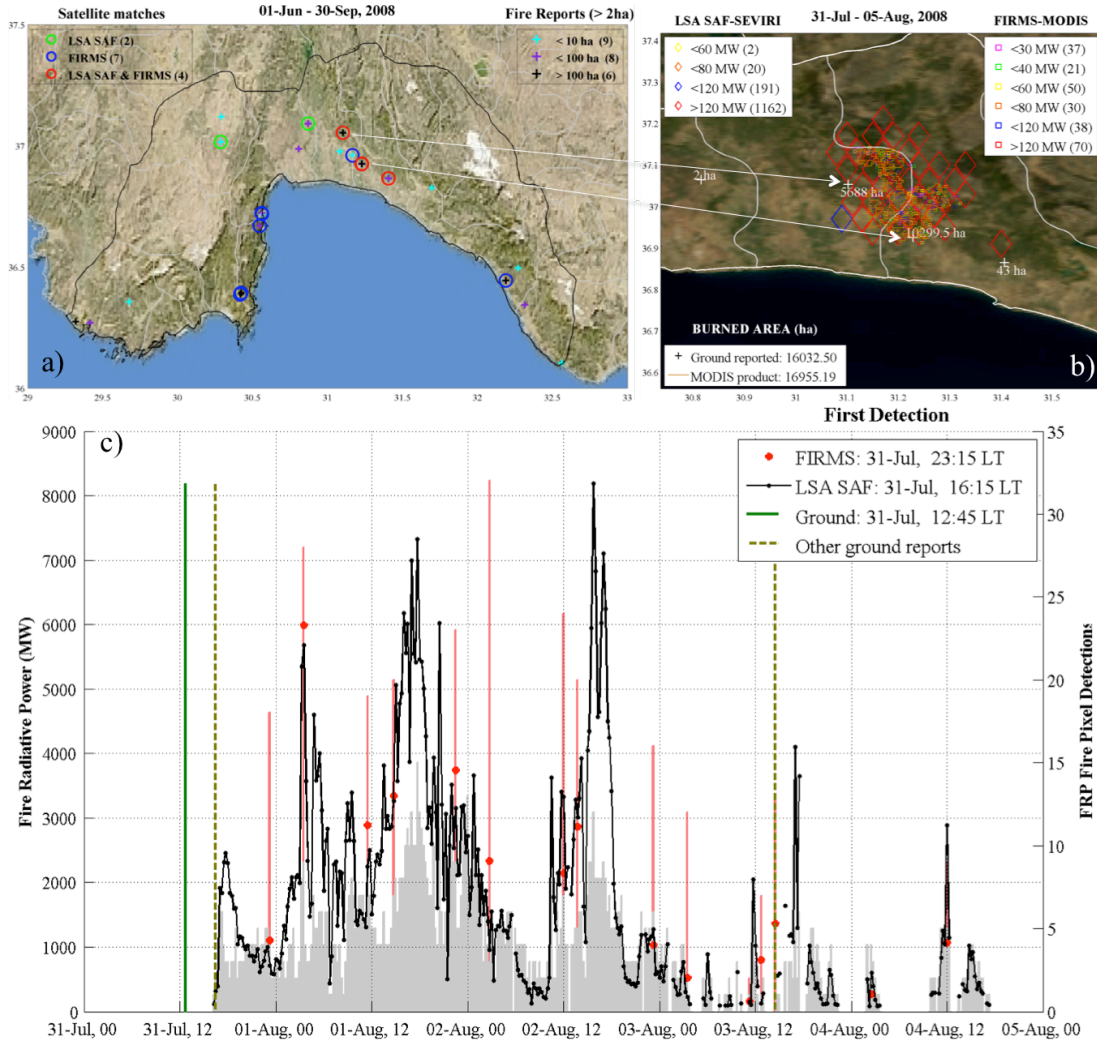


Figure 21. a) See Fig.18. b) Reported, FIRMS and LSA SAF fire pixels sorted by estimated FRP, for a large fire episode recorded in the municipalities of Taşagıl and Akbaş. Also the Burned Area product is included together with information of the ground recorded burned area. c) Total fire radiative power (FRP) recorded by FIRMS and LSA SAF (left axes) for the selected episode and number of fire pixels detected for each acquisition slot (left axes). Ground reported start time of the selected episode and others episodes recorded in the same spatiotemporal interval is also included (dark and light green lines).

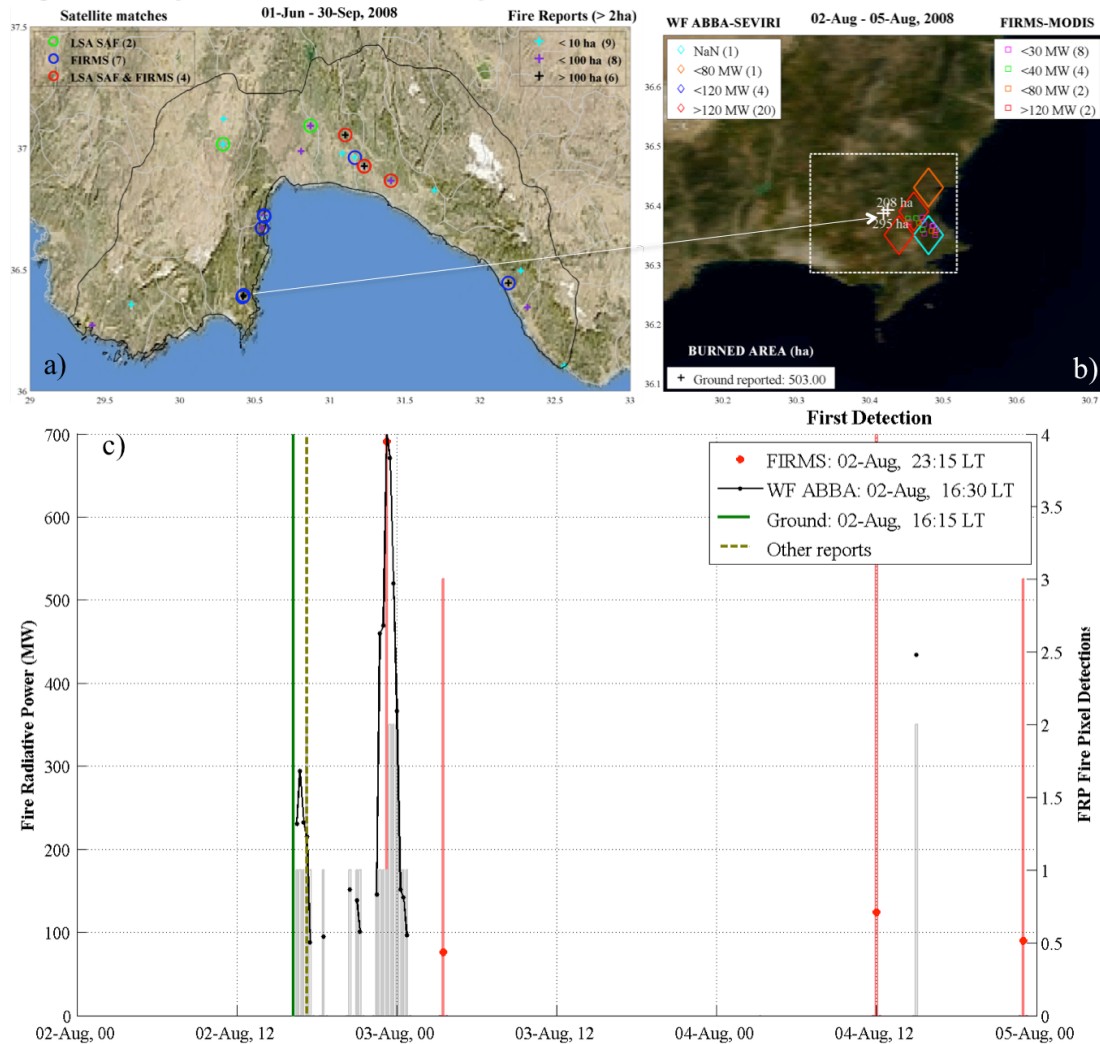


Figure 22. a) See Fig.18. b) Reported, FIRMS and WF ABBA fire pixels sorted by estimated FRP, for a large fire episode recorded in the municipalities of Yazır. Also information of the ground recorded burned area is included. 0.1x0.1-degree dashed box surrounding the municipality where the fire was detected is also depicted. c) Total fire radiative power (FRP) recorded by WF ABBA and FIRMS (left axes) for the selected episode and number of fire pixels detected for each acquisition slot (left axes). Ground reported start time of the selected episode and others episodes recorded in the same spatiotemporal interval is also included (dark and light green lines).

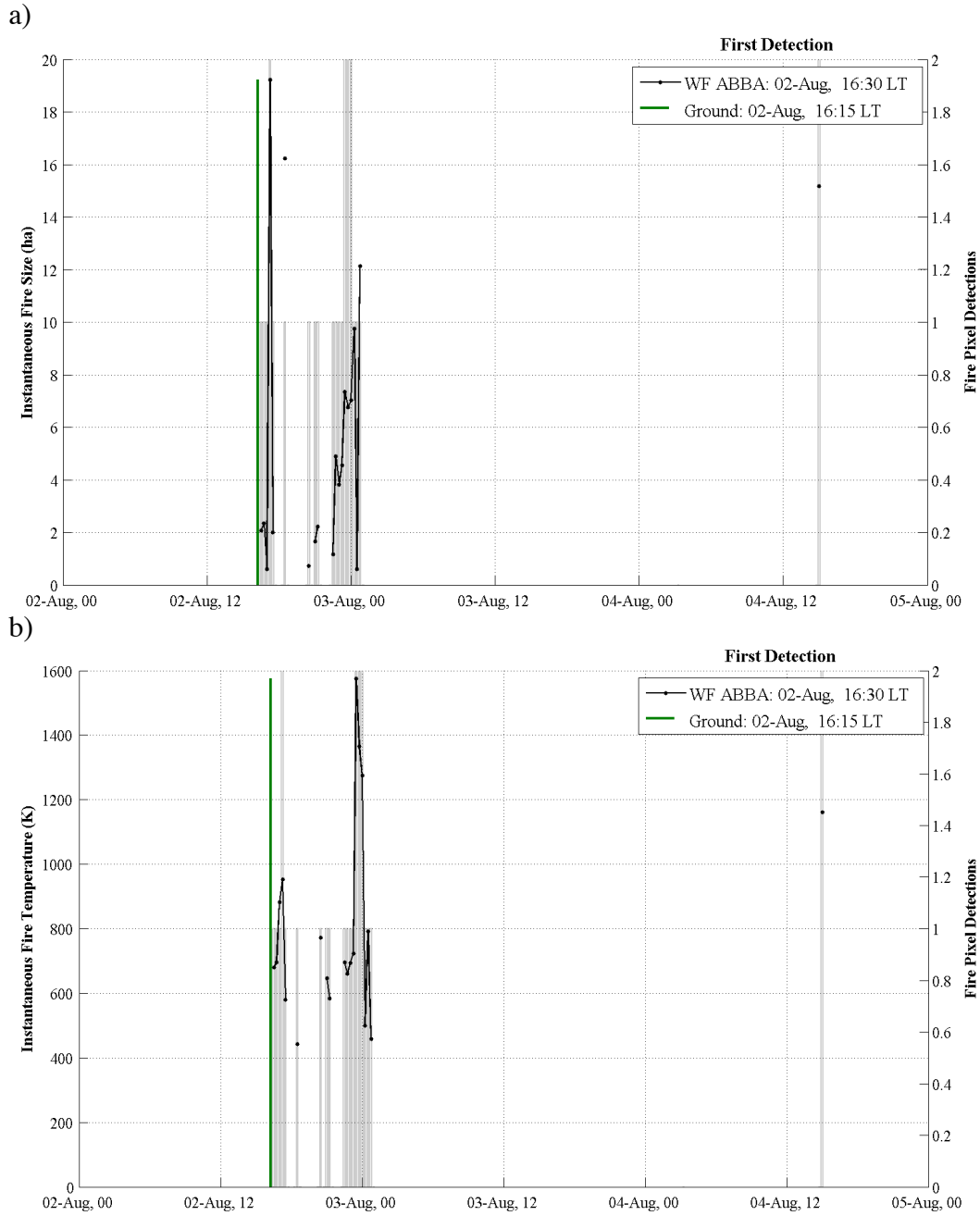


Figure 23. WF ABBA Instantaneous fire size and temperature for the episode described in Figure 22, recorded in the municipalities of Yazır. a) “Instantaneous Fire Size” (left axes) and number of fire pixels detected for each acquisition slot (left axes). b) “Instantaneous Fire Temperature” (left axes) and number of fire pixels detected for each acquisition slot (left axes). Ground reported start time of the selected episode and others episodes recorded in the same spatiotemporal interval is also included (dark and light green lines).

4.4. Describing large fires reported by the European Fire Information System

The European Forest Fire Information System (EFFIS) has been established by the European Commission to support the services in charge of the protection of forests against fires in the European Union and neighbor countries.

EFFIS provides fire assessment from pre-fire to post-fire phases, thus supporting fire prevention, preparedness, fire fighting and post-fire evaluations.

According to the 2008 EFFIS fire report, during this year the large forest damage in Europe occurred in the southeastern Mediterranean countries, which were under the influence of extreme weather conditions conducive to fire ignition and spread. The country most heavily damaged was Turkey, where the forest fire danger was high during the period of May to October, and the period of July to September was especially active due to very high temperatures, very low humidity and effective winds (Fig. 24). In Turkey, the coastline, which starts from Hatay and extends over the Mediterranean and Aegean up to Istanbul, has the highest fire risk. Approximately 60% (12 million ha) of Turkey's forest area is located in this fire sensitive area (JRC, 2009).

Fig. 25 shows the spatial location of the burned areas over Turkey as estimated by EFFIS in 2008. Only large fires (burned area more than 30 ha) are reported in EFFIS dataset, because the estimation of the burned area foresees the following steps:

- The use of auxiliary data like the news and the thermal anomalies detected by the MODIS satellite (MOD-14 products).
- The use of automatic processes (like the maximum likelihood classification).
- The final perimeter of the burnt area is acquired thorough photointerpretation using all the above mention data as auxiliary information over the MODIS images, channels 1 and 2 (250 meters resolution) and channel 7 (500 meters resolution resampled to 250 m).

In Fig. 26 and Fig. 27, all the reported fires are described in a similar fashion as done in the previous paragraph. We excluded the fires detected in the province of Antalya, already described above.

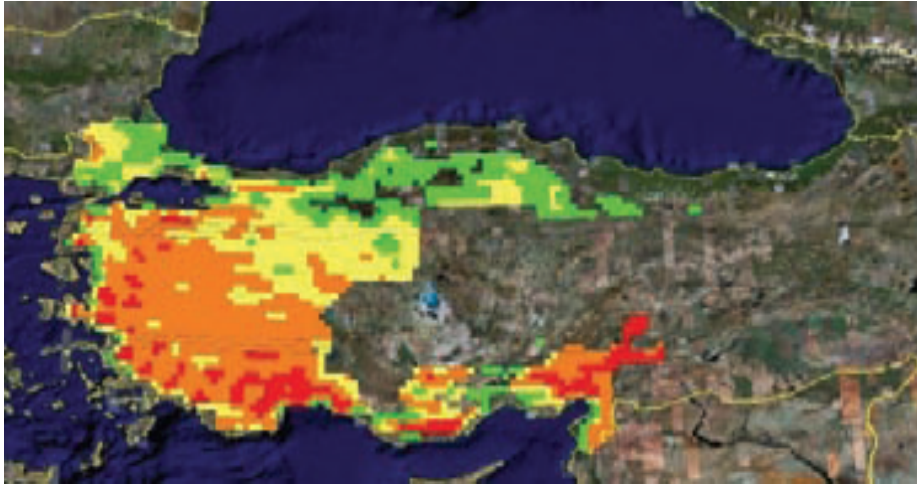


Figure 24. Fire danger level in Turkey during summer 2008 (EFFIS 2009).

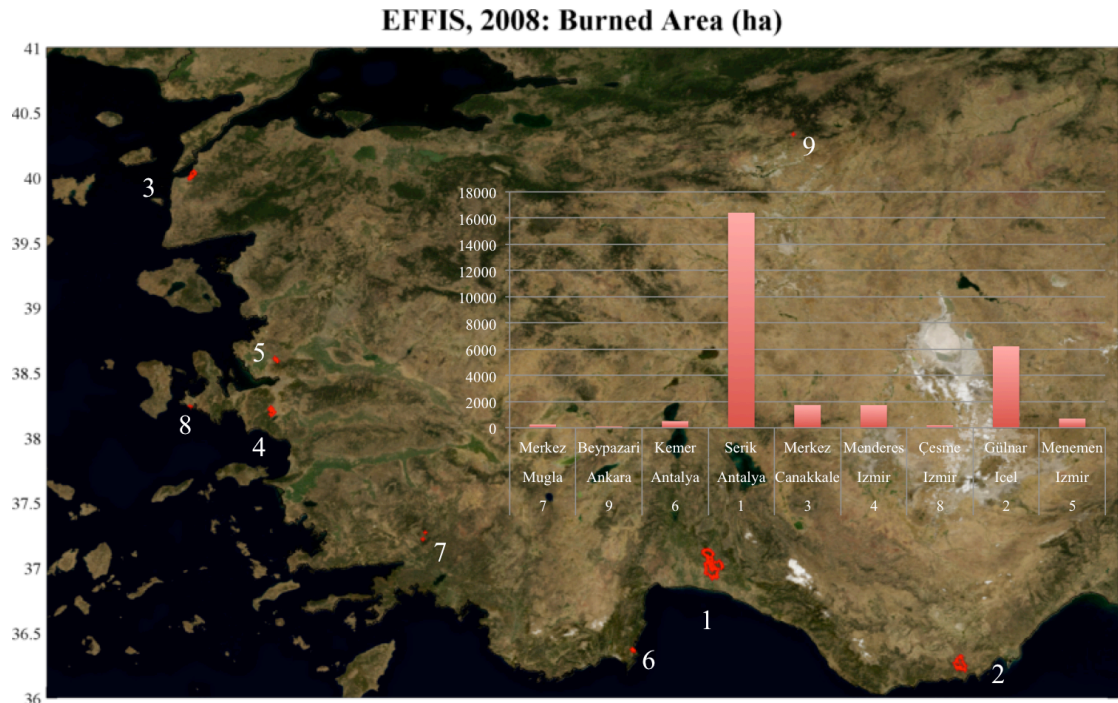


Figure 25. Burnt scars produced by forest fires in Turkey during the fire season 2008 (as estimated by EFFIS).

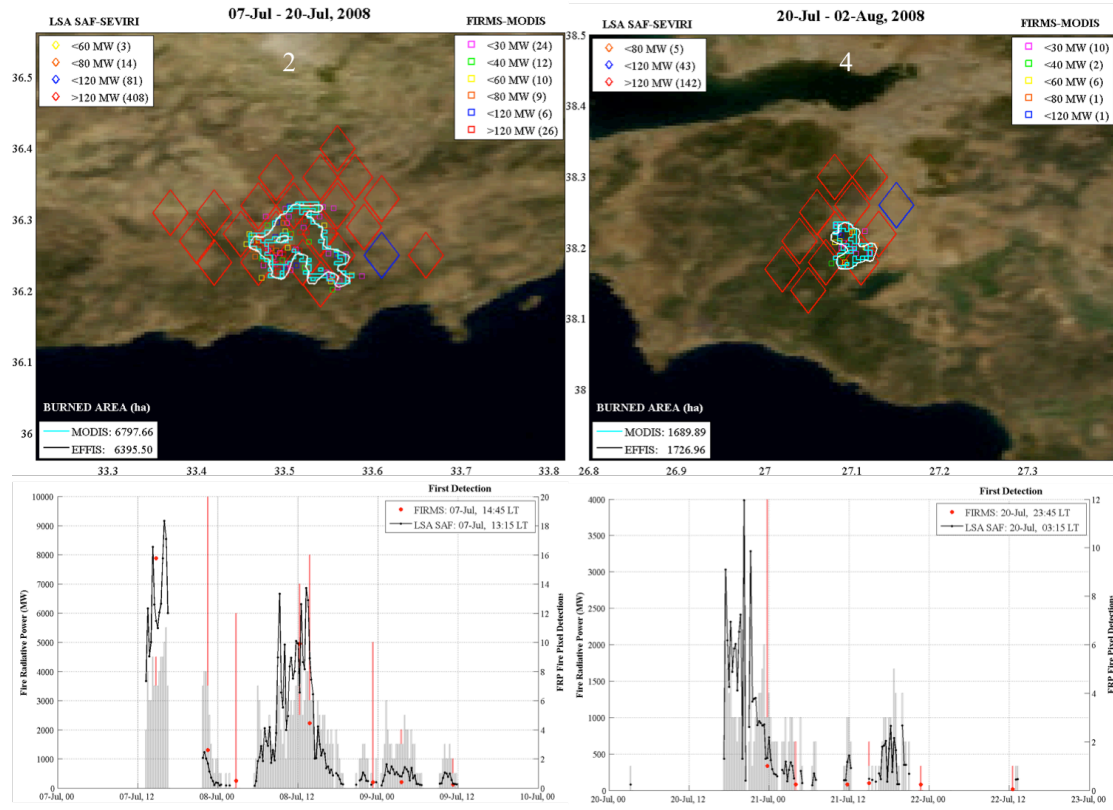


Figure 26. Upper panels. FIRMS and LSA SAF fire pixels sorted by estimated FRP, for the fire episodes recorded by EFFIS in 2008 (Fig. 25). MODIS and EFFIS estimated Burned Area product is included.

Lower panels. Total fire radiative power (FRP) recorded by FIRMS and LSA SAF (left axes) for the selected episode and number of fire pixels detected for each acquisition slot (left axes).

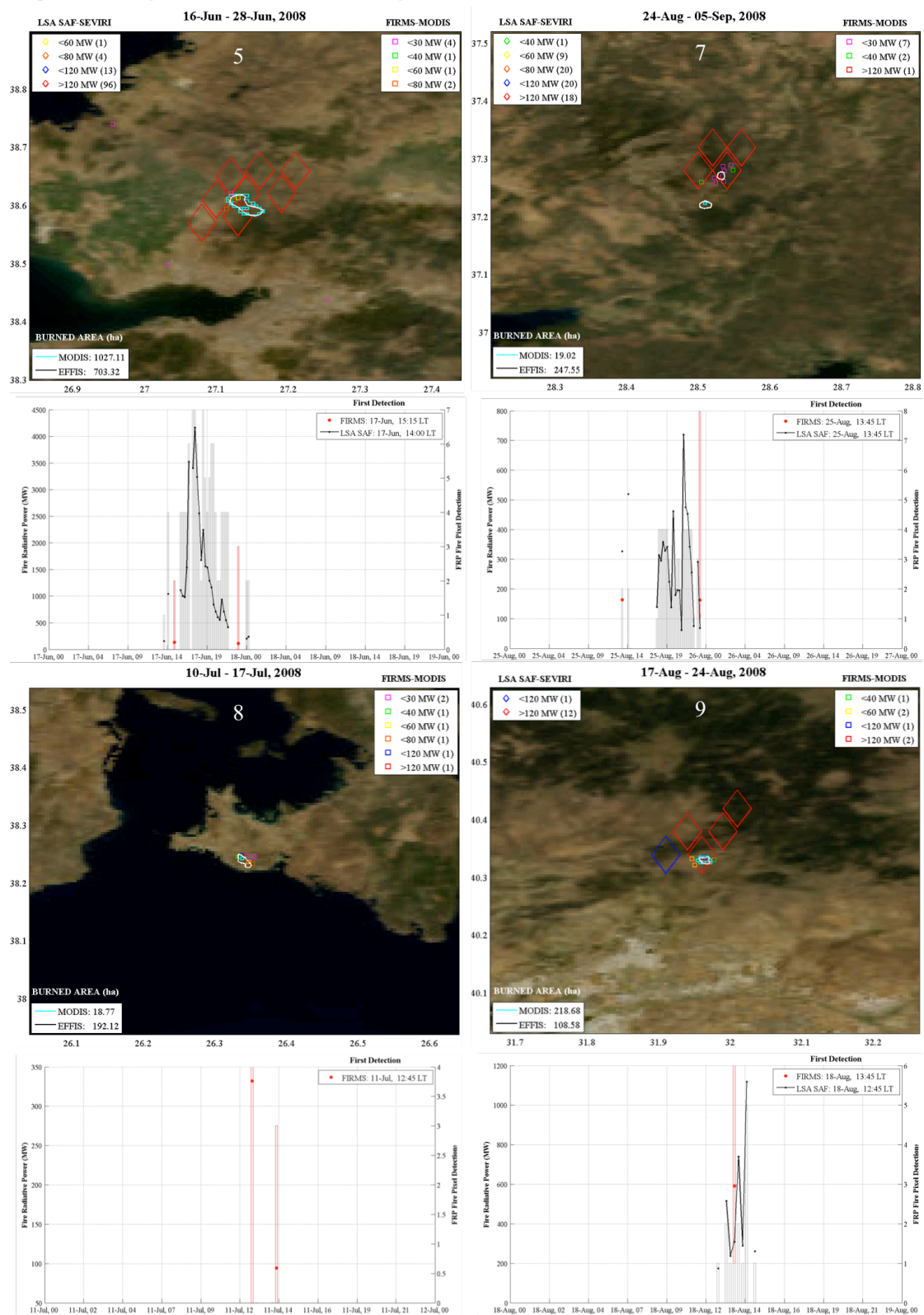


Figure 26. Continued.

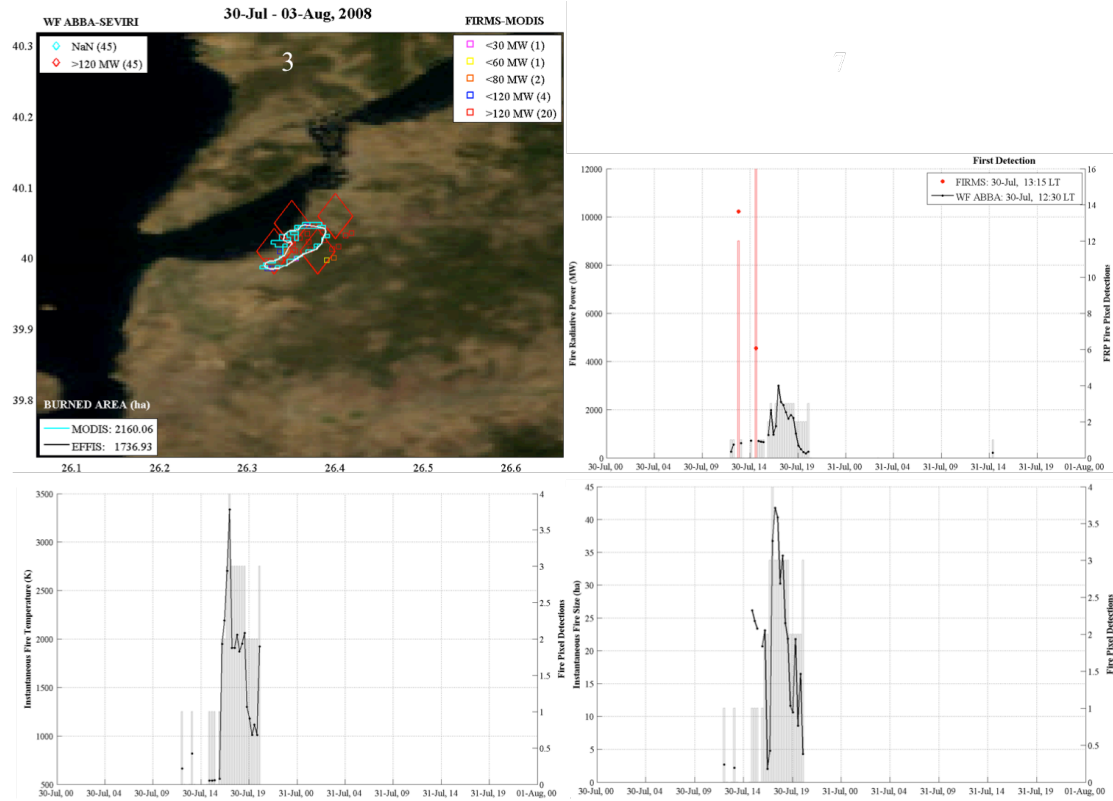


Figure 27. Upper right panel: FIRMS and WF_ABBA fire pixels sorted by estimated FRP, for a large fire episode recorded by EFFIS (Fig. 25) in 2008. MODIS and EFFIS estimated Burned Area product is included. Upper left panel: Total fire radiative power (FRP), recorded by FIRMS and WF_ABBA (left axes) for the selected episode and number of fire pixels detected for each acquisition slot (left axes). Lower panels: “Instantaneous Fire Temperature” (left) and “Instantaneous Fire Size” (right) as estimated by WF_ABBA.

4.5. MODIS Burned Area Product (Roy et al., 2005)

Fig. 28 shows the spatial distribution of the MODIS 500m Burned area collected between July 1 and September 30, 2008, over the province of Antalya together with the concurrent ground reported fires.

As mentioned before, the MODIS Burned Area Product allows detail mapping of fires of 50 ha or larger. Of the 6 reported fires with size larger than 100 ha, only 4 are unique events. Of these 4 events, 3 are identified by the selected burned area product and listed in Table 4. For the first two fires the satellite estimation of the burned area is very close to the ground one.

From Fig. 28, we can also notice that MODIS observed two burn scars that are not reported in the Ministry files.

Fig. 29 shows how the MODIS Burned Area Product describes the largest of the reported fires, occurred in the municipalities of Taşağıl and Akbaş, between July 31 and August 8, 2008. This product is able to provide us the daily burned area over the region affected by the fire at 500 meters resolution. The fire occurred in area forest mainly dominated by Turkish red pine (a typical fire adapted species of eastern Mediterranean basin ecosystems) and affected 17146 ha according to these data. In Figure 29, it is also shown, as a white outline, the burned area perimeter reported by the Forest Fire Brigades that encompass 20615 ha; this value is also different from the one reported in the official fire records, of 15987.5 ha, respectively 10299.50 ha for the municipality of Taşağıl and 5688 ha for the one of Akbaş. And, as black outline, the 2008 burned area perimeter extracted from the EFFIS database that encompass 16407 ha. The MODIS estimation correctly ranges over these values.

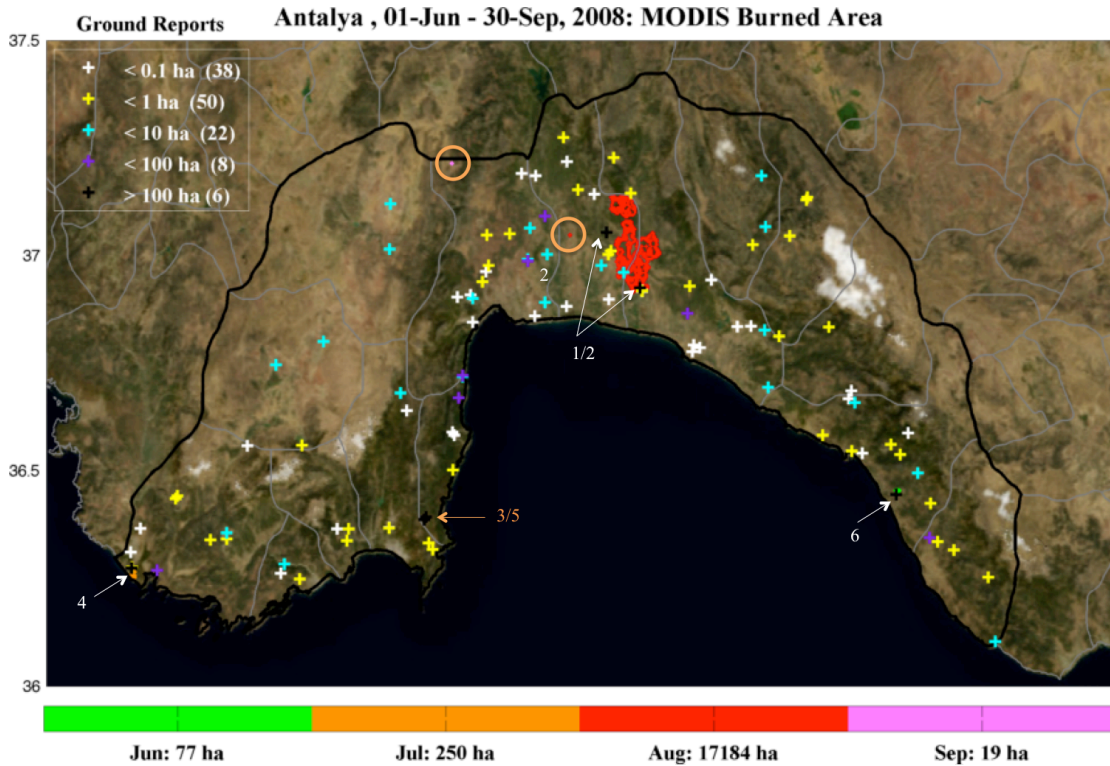


Figure 28. MODIS 500m burned area collected between July 1 and September 30,

2008, over the province of Antalya together with the concurrent ground reported fires. Ground reported fire, collocated with MODIS burned area, are identified by an arrow and their ID number (as in table 1) and listed in table 4. An orange arrow identifies the only reported fire with size larger than 100 ha not reported by MODIS burned area. On the contrary orange circles identify MODIS burned areas not reported by the Ministry of Forestry.

ID	Ministry of Forestry		MODIS Burned Area (ha)
	Location	Burned Area (ha)	
1	Taşağıl Belediyesi	10299.50	17107.83
2	Akbaş Köyü	5688.00	
4	Patara	210.00	269.64
6	Aliefendi Köyü	114.00	76.84

Table 4. Burned area of 3 large fires as reported by the Forest Fire Brigades and MODIS Burned Area Product. The first two reported fires refer to the same episode and the sum of their total burned area should be considered against the MODIS estimated one.

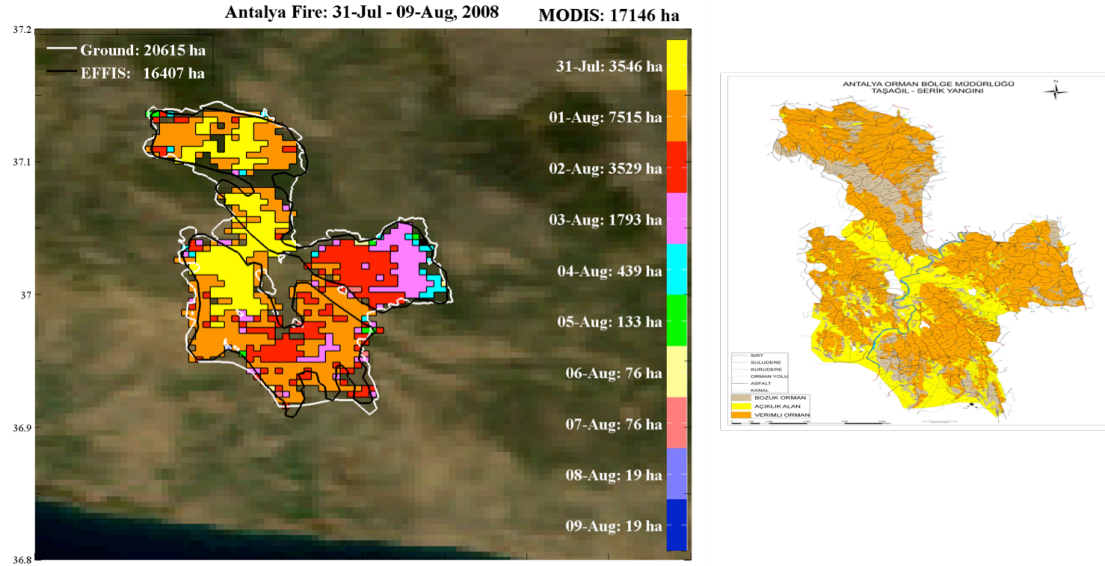


Figure 29. The large fire recorded in the municipalities of Taşağıl and Akbaş (ID 1 and 2 in Table 3), as viewed by the MODIS 500m burned area collected between July 31 and August 9, 2008 and coloured by day of the year they were detected. The fires occurred in areas forest, mainly dominated by Turkish red pines (*Pinus brutia*) and affected **171.5 km²** according to these data. Also shown as a white outline the ground reported burned area, of around **206 km²** and, as a black outline, the 2008 burned area perimeter extracted from EFFIS that encompass **164 km²**. The background is a MODIS Blue Marble image (500m resolution).

5. Summary and Conclusions

Forest fire is the most important factors that threaten forests in Turkey where the coastline, which starts from Hatay and extends over the Mediterranean and Aegean up to İstanbul, has the highest fire risk. Approximately 60% (12 million ha) of Turkey's forest area is located in fire sensitive areas. Every year in Turkey burn an average of 100 km² of Forest Land (JRC (2009)).

Satellite remote sensing technology provides the only automated fire detection method capable of detecting fire locations over large areas. For over 30 years meteorological and environmental satellites have been utilized to detect, monitor, and characterize fires.

The most used fire products have been traditionally based on polar-orbiting sensor data, mainly thanks to their high spatial resolution and acquisition at a global scale. But the most important limitation of polar satellite systems, with regard to the needs of continuous and in-real-time monitoring of wildfires, is their infrequent overpasses, varying inversely with the spatial resolution of the sensor. In this respect only geostationary systems with their inherent high temporal resolution can be helpful.

In this study we produced a performance analysis comparing the fire detections reported by the most stable polar (FIRMS-MODIS) and geostationary (LSA SAF-SEVIRI and WF_ABBA-SEVIRI) satellite fire products against the available ground truth over the province of Antalya, during the period June – September 2008. The major limitation of the available ground dataset is the absence of the exact geolocation and the duration of the observed fire episodes. Also a record of cloud cover is an important information to have when cross validating ground and satellite data.

According to recent publications (Koltunov et al., 2012), it is not reasonable to expect detection of wildfires from geostationary satellites that did not burn more than 2 ha over their lifetime. Over the province of Antalya during summer 2008, official reports with a total burned area larger than 2 ha are 23 out of 124 total. Combined, the LSA

SAF and FIRMS products detected 13 out of 23 fires in this category. Out of the 10 fires undetected by satellite, 9 were located in pixels classified as cloud or cloud edges or in pixels surrounded by pixels with these flags at its start time. Only one, the smallest of them, went undetected in condition of clear sky at its start time. The main limitation of the LSA SAF product for the selected case study is the fact that its Flag Quality product filters out large forested areas, flagged as coast line pixels.

This study shows that satellite detection and characterization of active fires can provide crucial information to Civil Protection Service and Forest Service in order to better manage wildfire control in terms of:

- Minimize the response time to the event.

In our study, 3 out of the 13 matching events were detected from satellite in less than 30 min from the first ground report. This is a good result if we consider that the study area is one of most touristic of Turkey and during the summer time is more densely populated. In the mobile phone era, in densely populated area, fires are normally reported shortly after they start. Therefore, only for a small fraction of wildfires can satellite observation provide the earliest alarm for this region.

Timely and reliable detection of active fires is particularly crucial for effective wildfire management, particularly in largely inaccessible mountainous areas. In these cases, satellite observations are luckily to provide us with the first announcement of fire occurrence in the area.

- Fire crisis management.

In our study, the geolocation of the active satellite pixel detections and the representation of the instantaneous energy liberated by the fire, the so called fire radiative power (FRP), (size and temperature in the case of WF-ABBA) shows that satellite observations make it possible to quickly locate and monitor large burning areas providing a synoptic picture of the burnings. Near real time monitoring and tracking of active fronts is very important during crisis management concerning the optimal distribution of ground and aerial forces.

It is important for decision makers to be aware that satellites can be used to continuously monitor biomass burning. To achieve even a fraction of the satellite fire

product coverage in remote areas with continual monitoring by ground and aircraft observations quickly becomes more expensive than satellite monitoring. The role of satellite observations for the management of forest fires has considerably increased during the last twenty years and it is intended to increase as the spatial, spectral and temporal characteristics of the sensors are constantly improving, as well as the techniques for the exploitation of satellite data. For example the next generation of Meteosat (MTG) will provide 1 km spatial resolution observations at 15 min intervals. We expect this to significantly reduce the latency of the satellite detections over Turkey.

REFERENCES

Arino, O., J. M. Rosaz, and P. Goloub. "The ATSR World Fire Atlas- A synergy with 'Polder' aerosol products." *Earth observation quarterly* 64 (1999): 1-6.

Amraoui, M, DaCamara, C.C., Pereira, J.M.C., (2010) Detection and Monitoring of African vegetation fires using MSG-SEVIRI imagery. *Remote Sensing of Environment*, 114, pp 1038-1052.

Ansey, T., Grégoire, K., Defourny , J., Leigh., P., Pekel, R., Van Bongaert., J., Artholomé, E., 2008, A new, global, multi-annual (2000–2007) burnt area product at 1 km resolution. *Geophysical Research Letters*, 35, L01401, doi: 10.1029/2007GL031567.

C Hang , D. and S ong , Y., 2009, Comparison of L3JRC and MODIS global burned area products from 2000 to 2007. *Journal of Geophysical Research*, 114, D16106, doi:10.1029/2008JD011361.

Calle, A., Casanova, J-L. and Gonzales-Alonso, F. (2009) Impact of point spread function of MSG SEVIRI on active fire detections. *International Journal of Remote Sensing*. 30.17.4567-4579.

Deeming, J.E., Burgan, R.E., Cohen, J.D. 1977. *The National Fire Danger Rating System 1978*, USDA For. Serv., Intermt. For. Range Exp. Stn., Ogden, Utah, Gen.



ŞZD REKLAM ve Org. GIDA İNŞ. PAZ. SAN. TİC. LTD. ŞTİ.

Tech. Rep. INT-39.

Dozier, Jeff. "A method for satellite identification of surface temperature fields of subpixel resolution." *Remote sensing of Environment* 11 (1981): 221-229.

European Commission (EC), 2009, *Forest Fires in Europe 2008*, EUR 23971 EN, Office for Official Publications of the European Communities, Luxembourg. p. 83

European Commission (EC), 2011, *Forest Fires in Europe 2010*, EUR 24910 EN, Office for Official Publications of the European Communities, Luxembourg. p. 85

European Commission (EC), 2013, *Forest Fires in Europe Middle East and North Africa 2013*, EUR 26791 EN, Office for Official Publications of the European Communities, Luxembourg. p. 107

FAO, 2008: *Workshop on Forest Fires in the Mediterranean Region: Prevention and Regional Cooperation*. Sabaudia, Italy, 13-15 May 2008. [Available online at: <ftp://ftp.fao.org/docrep/fao/010/k2891e/k2891e00.pdf>]

Georgiev, C.G., Stoyanova, J.S. (2013) Parallel use of SEVIRI LSA SAF FRP and MPEF FIR products for fire detection and monitoring. 2013 EUMETSAT Meteorological Satellite Conference. Oceanography and Climatology Conference. 16 th -20 th September. 2013. Vienna. Austria. ISSN 1011-3932

Giglio, Louis, et al. "An enhanced contextual fire detection algorithm for MODIS." *Remote sensing of environment* 87.2 (2003): 273-282.

Giglio , Louis, 2010, *MODIS collection 5 active fire product user's guide version 2.4*. Available online at: http://modis-fire.umd.edu/AF_usermanual.html

Joro, S., Samain, O., Yildirim, A., van de Berg, L. and Lutz, H. J. (2008) *Towards an improved active fire monitoring product for MSG satellites*.

JRC: *Forest Fires in Europe 2008*. JRC Scientific and Technical Reports, Tech. Rep. EUR 23971, Joint Research Centre, Ispra, Italy, available at: http://forest.jrc.ec.europa.eu/media/cms_page_media/9/forest-fires-in-europe-2009.pdf (last access: 2 December 2015), 2009.

Koltunov, A., Ustin, S. L., and Prins, E. M.: On timeliness and accuracy of wildfire detection by the GOES WF-ABBA algorithm over California during the 2006 fire season, *Remote Sens. Environ.*, 127, 194–209, 2012.

Laneve, G., Castronuovo, M.M., Cadau, E.G., (2006) Continuous Monitoring of Forest Fires in Mediterranean Area Using MSG. *Transactions on Geoscience and Remote Sensing, IEEE*, Oct. 2006, 44, 10, Part 1.

Luke, R.H., McArthur, A.G., 1978. *Bushfires in Australia*. Canberra, CSIRO Div. For. Res., Australian Gov. Publ. Serv.

Roy, D.P., Boschetti, L., Justice, C.O., Ju., J, The Collection 5 MODIS Burned Area Product - Global Evaluation by Comparison with the MODIS Active Fire Product, 2008. *Remote Sensing of Environment*, 112, 3690-3707.

Roy, D.P., Jin, Y., Lewis, P.E., Justice, C.O. 2005. Prototyping a global algorithm for systematic fire-affected area mapping using MODIS time series data. *Remote Sensing of Environment*, 97:137-162.

Roberts, G.J., Wooster, M.J., (2008) Fire Detection and Fire Characterization Over Africa Using Meteosat SEVIRI. *IEEE TRANSACTION on Geoscience and Remote Sensing*, 46, 4, pp 1200-1218.

Sifakis, N. I., Iossifidis, C., Kontoes, C., and Keramitsoglou, I.: Wildfire detection and tracking over Greece using MSG-SEVIRI satellite data, *Remote Sens.*, 3, 524–538, 2011. 7

Stocks, B.J., Lawson, B.D., Alexander, M.E., Van Wagner, C.E., McAlpine, R.S., Lynham, T.J., Dube, D.E., 1989. Canadian Forest Fire Danger Rating System: an overview. *Forestry Chronicle* 65: 258 265

Tramutoli, V., (2007) Robust Satellite Techniques (RST) for Natural and Environmental Hazards Monitoring and Mitigation: Theory and Applications. *Proceedings of Multitemp 2007*, DOI 10.1109/MULTITEMP.2007.4293057.

Wooster, M. J., Roberts, G., Freeborn, P. H., Xu, W., Govaerts, Y., Beeby, R., He, J.,



3ZD REKLAM ve Org. GIDA İNŞ. PAZ. SAN. TİC. LTD. ŞTİ.

Lattanzio, A., and Mullen, R.: Meteosat SEVIRI Fire Radiative Power (FRP) products from the Land Surface Analysis Satellite Applications Facility (LSA SAF) – Part 1: Algorithms, product contents and analysis, *Atmos. Chem. Phys. Discuss.*, 15, 15831–15907, doi:10.5194/acpd-15-15831-2015, 2015.

Wooster, M.; Zhukov, B.; Oertel, D. Fire radiative energy for quantitative study of biomass burning: Derivation from the BIRD experimental satellite and comparison to MODIS fire products. *Remote Sens. Environ.* 2003, 86, 83–107.